ACCSCIENCE PUBLISHING

International Journal of Bioprinting

REVIEW ARTICLE

Three-dimensional bioprinting in human-relevant toxicology: Advanced organ models and translational strategies

Yinpeng Le[1,2], Tanqing Long[2,3], Qi Wang[2], Mengcheng Tang[1], Mingyue Pan[2,4], Qingru Song[2,5], Wenrui Ma[5], Yuxin Su[2], Yutian Feng[2], Ni An[5], Wenzhen Yin[5], Xiangdong Kong[1]*, Yunfang Wang[2,5,6]*, and Juan Liu[2,6]*

[1]Zhejiang-Mauritius Joint Research Center for Biomaterials and Tissue Engineering, School of Materials Science and Engineering, Zhejiang Sci-Tech University, Hangzhou, Zhejiang, China

[2]Hepato-Pancreato-Biliary Center, Beijing Tsinghua Changgung Hospital, School of Clinical Medicine, Tsinghua Medicine, Tsinghua University, Beijing, China

[3]Department of Pharmacology, School of Pharmacy, Tongji Medical College, Huazhong University of Science and Technology, Wuhan, Hubei, China

[4]State Key Laboratory of Natural Medicines and Jiangsu Key Laboratory of Drug Discovery for Metabolic Diseases, Center of Advanced Pharmaceuticals and Biomaterials, China Pharmaceutical University, Nanjing, Jiangsu, China

[5]Clinical Translational Science Center, Beijing Tsinghua Changgung Hospital, Tsinghua Medicine, Tsinghua University, Beijing, China

[6]Ministry of Education Key Laboratory of Digital Intelligence Hepatology, School of Clinical Medicine, Tsinghua Medicine, Tsinghua University, Beijing, China

***Corresponding authors:**
Juan Liu
(lja02720@btch.edu.cn)

Yunfang Wang
(wangyf008@mail.tsinghua.edu.cn)

Xiangdong Kong
(kongxd@zstu.edu.cn)

Citation: Le Y, Long T, Wang Qi, *et al.* Three-dimensional bioprinting for human-relevant toxicology: Advanced organ models and translational strategies. *Int J Bioprint*. 2025;11(4):99-132. doi: 10.36922/IJB025210209

Received: May 21, 2025
Revised: June 25, 2025
Accepted: July 3, 2025
Published online: July 3, 2025

Abstract

Traditional toxicological testing, which relies on animal models and two-dimensional cell cultures, encounters challenges in accurately predicting human-specific responses due to interspecies variability and the inherent limitations of simplified *in vitro* systems. Three-dimensional (3D) bioprinting has emerged as a transformative approach, facilitating the fabrication of physiologically relevant tissue constructs with precise spatial control over cellular and extracellular matrix components. This review critically examines recent advancements in 3D-bioprinted organ models, such as the liver, kidney, and lung, for toxicological assessments, including their applications in drug safety evaluation, environmental pollutant screening, and nanomaterial risk assessment. We further analyze persistent technical barriers concerning resolution limitations, material biocompatibility, and the simulation of multi-organ interactions. Finally, we propose integrative strategies that combine organ-on-a-chip platforms, artificial intelligence-driven design, and standardized validation protocols, aiming to accelerate the translational potential of bioprinted models in regulatory toxicology.

Keywords: Functional simulation; Organ models; Three-dimensional bioprinting; Toxicology testing

1. Introduction

Toxicity arises from adverse biological events triggered by exposure to biological, physical, or chemical agents and manifests as reversible or irreversible dysfunctions, ranging from transient cellular perturbations to severe organ failure and mortality.[1] These outcomes are governed by the interplay between the absorption, distribution, metabolism, and excretion (ADME) properties of toxicants, as well as their interactions with cellular macromolecules.[2] Toxicology, as the scientific discipline dedicated to evaluating toxicity mechanisms, severity, and frequency, has evolved into a cornerstone of modern pharmacology and chemical safety assessment.[3] However, the escalating demand for toxicity testing, fueled by the annual introduction of over 2000 new chemicals across pharmaceuticals, cosmetics, and industrial sectors, has revealed critical limitations in conventional approaches.[4]

Historically, animal testing served as the gold standard for toxicological evaluations.[5] Although these models provide preliminary safety data, interspecies physiological disparities, such as divergent ADME profiles, metabolic pathways, and lifespans, severely undermine the translatability of animal-derived results to humans.[4] For instance, between 38% and 51% of drug-induced liver injuries remain undetected during preclinical animal trials, culminating in costly late-stage clinical failures or post-market withdrawals.[6] Beyond ethical concerns, animal models are characterized by low throughput, prolonged testing cycles, and high operational costs, prompting an urgent need for human-relevant alternatives.[7]

The "Replacement, Reduction, Refinement" (3R) principles have catalyzed a paradigm shift toward *in vitro* systems.[8–10] The global *in vitro* toxicology testing market, valued at USD 10.1 billion in 2022, is projected to reach USD 17.1 billion by 2028, indicating a compound annual growth rate of 9.5%.[11] Early *in vitro* models, including two-dimensional (2D) monocultures and static three-dimensional (3D) constructs, partially address ethical and throughput challenges; however, they fail to replicate the dynamic cell–cell and cell–extracellular matrix (ECM) interactions and tissue-level complexity of human organs.[12,13] For example, 2D-cultured hepatocytes rapidly dedifferentiate, losing cytochrome P450 activity within hours,[14,15] whereas conventional 3D spheroids often develop hypoxic cores due to inadequate nutrient diffusion. Organ-on-a-chip platforms, which integrate microfluidics and mechanical cues, represent a significant leap forward but encounter scalability issues and limited standardization.[7]

Three-dimensional bioprinting has emerged as a transformative technology to overcome these bottlenecks.[16] By enabling layer-by-layer deposition of living cells, biomaterials, and bioactive factors with micrometer-scale precision, bioprinting constructs physiologically relevant tissue architectures, such as vascularized liver lobules, polarized renal tubules, and alveolar-capillary barriers, that mirror native organ functionality.[17–20] Advanced bioinks, including gelatin methacryloyl (GelMA) and decellularized ECM (dECM)-based hydrogels, provide tunable mechanical properties and biochemical niches that maintain cell viability and phenotypic stability.[21] Integrated microfluidic channels ensure sustained oxygenation and nutrient supply, thereby resolving necrosis issues in thick tissues. Notably, bioprinted models exhibit enhanced predictive accuracy for organ-specific toxicities, as demonstrated by their ability to distinguish structural analogs such as trovafloxacin (hepatotoxic) and levofloxacin (non-toxic), a feat unattainable with traditional models.[22]

This review critically evaluates how 3D bioprinting addresses the limitations of existing *in vitro* toxicology models. We first delineate the research trends and the technological evolution from animal testing to organ-on-a-chip systems, highlighting ongoing challenges in physiological fidelity and scalability, as illustrated in Figure 1. Next, we analyze advancements in bioprinting modalities, such as extrusion, laser-assisted, and stereolithography, as well as bioink design and functional tissue fabrication. A central focus is placed on organ-specific applications, such as liver, kidney, and lung toxicity assessments, where bioprinted models outperform conventional approaches in replicating human pathophysiology. We also address unresolved controversies, including the lack of standardized validation protocols and regulatory acceptance barriers. By synthesizing interdisciplinary innovations in materials science, microfluidics, and artificial intelligence, this work aims to outline a roadmap for translating bioprinted platforms into mainstream toxicological practice.

2. A historical perspective on toxicological paradigms

2.1. The foundational era of toxicology

The nascent form of toxicology arose from rudimentary observations of natural phenomena and early experimental inquiries. In the 16th century, Paracelsus introduced the pivotal principle that "the dose makes the poison," thereby establishing the dose–response relationship as the cornerstone of toxicological science and laying the groundwork for subsequent research in the field.[23] By the late 18th century, British physician Percivall Pott's investigation into scrotal cancer among chimney sweeps

revealed the carcinogenic mechanisms of polycyclic aromatic hydrocarbons, marking the advent of modern toxicological studies.[24] In the early 19th century, French scientist Mathieu Orfila systematically validated the effects of toxins through animal experimentation, whereas Magendie and Claude Bernard explored neurotoxic mechanisms.[25–28] These pioneering studies laid the foundation for the experimental methodologies that underpin modern toxicology.

2.2. The era of animal model dominance

The application of animal models in toxicological research has undergone a significant evolution, evolving from preliminary investigations to routine applications. In 1927, J.W. Trevan, drawing upon Paracelsus's foundational principles, introduced the concept of the median lethal dose (LD_{50}). By employing statistical methodologies, Trevan defined LD_{50} as a universal benchmark for evaluating acute toxicity, laying the groundwork for future advancements in toxicity testing.[29,30] This innovation marked a pivotal shift from qualitative to quantitative toxicological analysis, providing a scientific basis for subsequent evaluations. By the mid-20th century, animal experimentation was established as the cornerstone of toxicological investigations.[31] The LD_{50} test was extensively utilized for categorizing the acute toxicity profiles of industrial compounds and pharmaceutical agents, serving as a vital tool for assessing chemical toxicity.[32,33]

Through animal experiments, researchers obtained foundational knowledge regarding the ADME of drugs, as well as their potential toxicities and adverse effects.[34] During this era, animal testing not only played a critical role in drug development but also supported the toxicity assessment of environmental pollutants. However, growing ethical concerns surrounding the extensive use of animal testing, particularly the ethical dilemmas associated with animal suffering, began to emerge. In 1959, the introduction of the 3R principle initiated a paradigm shift in ethical considerations for animal testing.[31] This principle advocated for minimizing animal usage through alternative methods and refining experimental procedures to alleviate animal suffering, steering toxicological research toward exploring efficient *in vitro* models and alternative approaches to reduce reliance on animal testing.[10]

Despite these ethical considerations, animal models remained integral to toxicological studies for decades.[35] They enabled researchers to simulate complex biological processes and evaluate the toxic effects of substances *in vivo*, providing indispensable support for drug development and environmental safety assessments.[36] Nevertheless, advancements in science and technology have spurred the emergence of *in vitro* models and computational simulations, offering additional options and potential avenues for reducing animal testing. Future research should continue to explore the application potential of these novel methods to facilitate sustainable progress in toxicological research.

2.3. Disruption in *in vitro* models: From cell cultures to organ simulation

Over an extended period, toxicological research principally depended on whole-animal experimentation and human observational studies. However, challenges in accurately replicating complex exposure scenarios, coupled with interspecies and individual variability between humans and various animal models, have impeded a holistic understanding of the toxicological effects of exogenous substances, complicating the research processes. Recent advancements in tissue engineering and molecular biology have facilitated the development of highly refined *in vitro* models that emulate human tissue functionality. These include widely utilized 2D and 3D cell culture systems, organoids, and microfluidic chips. Such innovations are progressively diminishing dependence on conventional animal-based approaches in toxicological research.

2.3.1. Two-dimensional monolayer culture

Two-dimensional cell cultures represent a classical *in vitro* model extensively employed in toxicological investigations. Originating from primary cell lines, cancer-derived cell lines, and stem cells, these systems have become indispensable tools in biological research since Harrison's groundbreaking achievement in animal cell culture in 1901.[37] The discovery of HeLa cells in 1951 initiated the extensive utilization of cancer cell lines as readily accessible experimental platforms.[38] Subsequent milestones included the successful isolation and establishment of mouse and human embryonic stem cell lines in 1981 and 1998, respectively.[39,40] Beyond cellular models, Bruce Ames' development of the bacterial reverse mutation assay in 1975, incorporating a liver microsomal metabolic activation system, enabled efficient high-throughput screening for carcinogenic substances, thereby reducing dependence on mammalian experimental systems.[41,42] In 2007, Zeiger[42] achieved a groundbreaking milestone by reprogramming human somatic cells to generate the first induced pluripotent stem cell (iPSC) lines.

Today, widely adopted 2D cell systems encompass human colorectal adenocarcinoma (Caco-2), Madin–Darby canine kidney (MDCK), human alveolar basal epithelial (A549), and bronchial epithelial (BEAS-2B) cell lines, which serve diverse applications in assessing the toxicity of chemicals, pharmaceuticals, and environmental pollutants. For instance, Caco-2 cells are extensively utilized to investigate intestinal absorption and drug

transport mechanisms,[43] MDCK cells are employed to study epithelial permeability in the intestine and kidneys,[43,44] A549 cells are used to evaluate the toxicity of inhaled substances and nanoparticles (NPs), while BEAS-2B cells remain instrumental in examining the respiratory toxicity of chemical agents.[45] The advantages of 2D cell cultures, including their high-throughput capability and cost-effectiveness, render them ideal for large-scale screening and initial toxicity assessments.[46] However, their limitations, such as alterations in cell morphology and functionality, insufficient barrier properties, and limited metabolic capacity, remain significant challenges that warrant careful consideration.[46,47] Advances such as gene editing, co-culture techniques, and optimized culture conditions have provided partial solutions to these inherent limitations. For example, MDCK cells' permeability and metabolic capabilities have been improved via gene transfection techniques that incorporate transport proteins and metabolic enzymes.[44] Similarly, Deguchi *et al.*[48] leveraged human iPSCs with genome editing to generate cytochrome P450 3A4-knockout iPSCs, which were subsequently differentiated into hepatocyte-like cells and intestinal epithelial-like cells. These models have yielded critical insights into cytochrome P450 3A4-mediated hepatic toxicity in early-stage drug development.

2.3.2. Three-dimensional static models

In conventional 2D cell cultures, cells exhibit adhesion patterns, spatial orientation, morphology, and polarity that substantially differ from their physiological states observed *in vivo*.[47] By contrast, 3D culture systems allow cells to adopt spatially organized arrangements, enabling the dynamic regulation of essential physiological processes across temporal and spatial dimensions, thereby facilitating the reconstitution of organ or tissue functionality.[49] Beyond serving as mere structural scaffolds, 3D culture systems are required to maintain the viability of cells, tissues, and organs by emulating physiological microenvironments, including soluble factor signaling, electrical signal transmission, and extracellular matrix-mediated mechanotransduction.[47,49] Increasingly, research highlights the ability of 3D cell models to reproduce *in vivo*-like cell morphology, thereby underscoring their applicability in toxicological investigations.

Early 3D culture approaches involved incorporating cells derived from animal tissues or immortalized human cell lines into hydrogel matrices.[50] For instance, Astashkina *et al.*[50] encapsulated mouse proximal tubular epithelial cells in hydrogel matrices, generating 3D cell models to evaluate endpoints such as cytochrome P450 activity, metabolite production, and kidney injury molecule-1 biomarker expression. Comparisons with 2D-cultured LLC-PK1 and HEK293 cells revealed that 3D proximal tubular epithelial cell models demonstrated biomarker profiles that more closely resembled *in vivo* observations. However, the study also noted a twofold decline in cell viability within 2 weeks, emphasizing a prevalent limitation associated with static 3D culture methodologies.

2.3.3. Organoids and organ-on-a-chip models

The rapid advancements in materials science and biology have driven the development of organoids and organ-on-a-chip technologies—two pioneering 3D culture systems that offer physiologically relevant models for toxicological research.[51] Organoids are self-organizing, 3D cellular structures originating from pluripotent, embryonic, or adult stem cells. These structures recapitulate the functional, structural, and biological complexity of specific organs, offering physiologically robust *in vitro* platforms for toxicological investigations. Since Sato *et al.*[52] successfully established the first intestinal organoid in 2009, organoid technology has evolved to include diverse organ systems, such as the stomach,[53] lung,[54] brain,[55] liver,[56] heart,[57] and kidneys.[58] In toxicological research, organoids offer unique advantages.[59] For example, airway organoids exposed to microplastic fibers can simulate real-world exposure conditions and developmental processes, highlighting phenomena like organoid encapsulation of microplastics, which are not observable in conventional 2D cell models.[60] This capability enables organoids to provide more accurate and sensitive insights into the impacts of harmful environmental factors on human health, serving as dependable platforms for toxicological evaluations.[7]

Organ-on-a-chip technology, based on microfluidic systems, represents a sophisticated platform for mimicking human organ functionality and drug response mechanisms *in vitro*. By precisely controlling fluid shear stress, mechanical strain, and co-culture conditions, these systems reconstruct organ-specific physiological microenvironments. Notably, organ-on-a-chip devices can simulate the functions of individual organs or integrate multiple chips to construct "body-on-a-chip" systems, facilitating explorations of inter-organ communication and pharmacokinetic dynamics. In toxicological evaluations, this technology holds substantial potential. For instance, lung-on-a-chip models can reproduce the complex and integrated organ-level responses of the lungs to bacteria and inflammatory cytokines introduced into the alveolar space. Meanwhile, the lung model reveals that cyclic mechanical strain exacerbates the toxicity and inflammatory response of the lungs to silica NPs.[61] Additionally, multi-organ chip systems provide a comprehensive framework for assessing

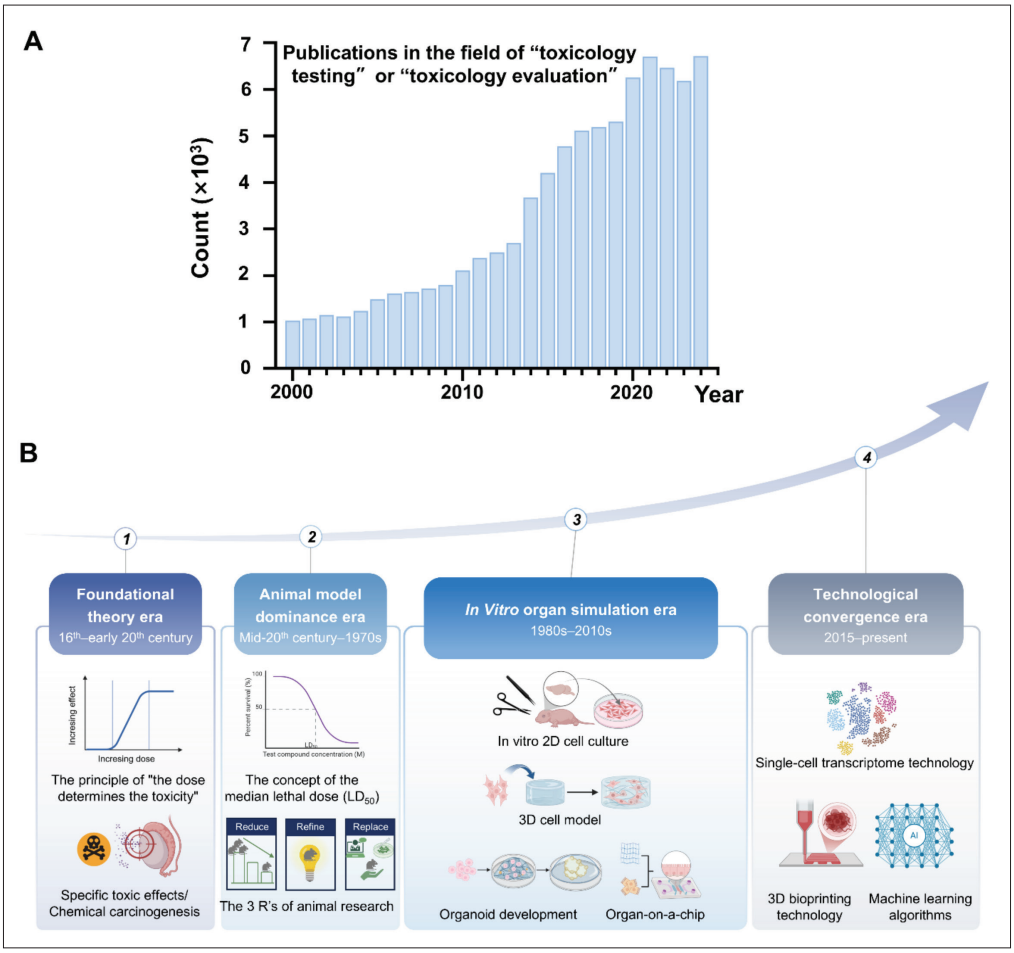

Figure 1. Technological evolution and research trends. (A) The exponential growth of PubMed-listed publications on "toxicology testing" and "toxicology evaluation" since 2000, reflecting the field's rapid transition toward engineered models. (B) Key milestones across four epochs: (i) foundational theory era (16th–early 20th century): dominated by observational studies and median lethal dose (LD_{50}) standardization, (ii) animal model dominance era (mid-20th century–1970s): emergence of cellular assays and early 3R-driven innovations, (iii) *in vitro* organ simulation era (1980s–2010s): rise of organoids and microphysiological systems, and (iv) technological convergence era (2015–present): integration of bioprinting, artificial intelligence-driven design, and multi-omics validation. Created with Biorender [û, NP. (2025). https://BioRender.com/mu9mwhw. Abbreviation: 3Rs, replacement, reduction, and refinement.

drug metabolism, distribution, and toxicity, improving the reliability and precision of toxicological predictions.[62]

2.4. The era of technological convergence: The emergence of precision and systems toxicology

Contemporary toxicological research is characterized by the convergence of multiple advanced technologies, prompting a paradigm shift from organ-specific evaluations to comprehensive system-level biological analyses. 3D bioprinting techniques, employing extrusion-based processes and sacrificial materials such as Pluronic F127, have facilitated the development of vascular networks, extending the viability of liver models to over 30 days while maintaining fluctuations in drug-metabolizing enzyme activity within 15%.[63–65] Photocuring technologies, with a resolution of 5 μm, have successfully replicated the spatial alignment of myocardial fibers, offering improved spatial precision for evaluating cardiac toxicity.[66,67] Single-cell transcriptomics has revealed the diverse responses of pulmonary epithelial cell subpopulations to NP exposure, such as the upregulation of inflammation-specific factors in basal cells.[68] Meanwhile, machine learning algorithms have integrated high-throughput *in vitro* data—including reactive oxygen species (ROS) generation and cell cycle arrest—to forecast organ-level toxicity *in vivo*.[69,70]

In 2022, the United States Food and Drug Administration released the "Strategic Roadmap for Alternative Methods," integrating organ-on-a-chip data as part of the evaluation framework for investigational new drug applications. Despite these advancements, challenges

such as establishing robust validation standards—such as achieving inter-laboratory reproducibility with error margins below 20%—and enhancing the functional maturity of vascular networks persist as areas requiring further attention.[71,72] This phase of technological evolution signifies a critical transition in toxicology, shifting from empirical threshold-based evaluations to system-wide perturbation analyses. Such developments establish a robust foundation for precision medicine and individualized toxicity forecasting.[73]

3. Three-dimensional bioprinting: Foundations and platforms for *in vitro* toxicological models

3.1. Modalities of bioprinting technology: Principles and parameter comparisons

The core of 3D bioprinting technology lies in the precise spatial arrangement of cells and biomaterials, where the selection of printing modalities critically impacts the physiological fidelity and functional sophistication of the generated models. Based on their operational principles, 3D bioprinting strategies are classified into extrusion-based bioprinting, photocuring-based bioprinting, inkjet bioprinting, laser-assisted bioprinting, and other emerging bioprinting modalities.

Extrusion-based bioprinting uses mechanical or pneumatic pressure to deposit high-viscosity bioinks through micro-nozzles. Thermoplastics via fused deposition modeling (FDM) or cell-compatible hydrogels via cold extrusion, as shown in Figure 2A and B, while photocuring approaches such as laser scanning stereolithography and digital light processing achieve subcellular resolution—by layerwise ultraviolet or visible-light crosslinking of methacrylated polymers, as shown in Figure 2C and D. Inkjet bioprinting utilizes thermal bubble or piezoelectric mechanisms to partition low-viscosity bioinks into microdroplets. This modality is categorized into drop-on-demand and continuous inkjet methodologies, as shown in Figure 2F and G. Laser-assisted methods like laser-induced forward transfer and absorption film-assisted laser printing transfer cell-laden bioinks with single-cell (~10 μm) precision while preserving viability,[74,75] as shown in Figure 2E. Emerging techniques—including suspended bioprinting in support baths for ultra-soft constructs, as shown in Figure 2H, and selective laser sintering of biocompatible powders for

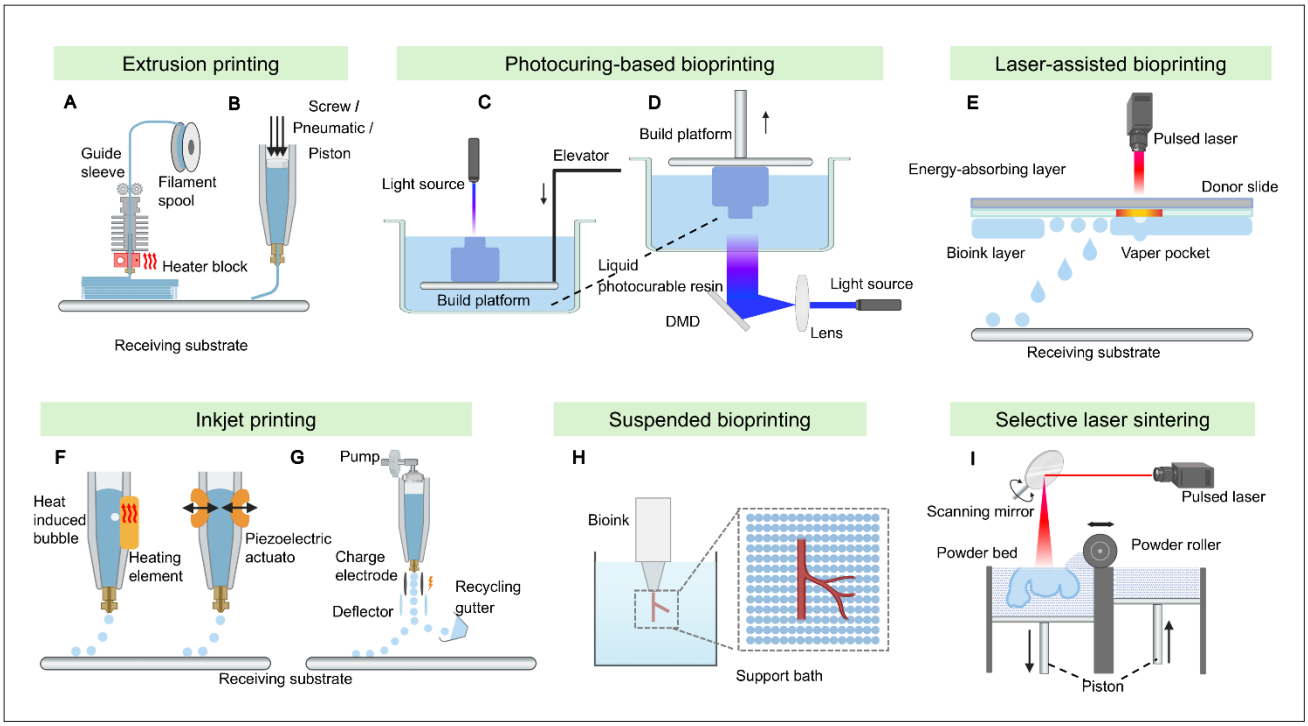

Figure 2. Common three-dimensional printing technologies in the biomedical field. (A) Fused deposition modeling. (B) Cold extrusion. (C) Laser scanning stereolithography. (D) Digital light processing. (E) Laser-assisted bioprinting. (F) Drop-on-demand inkjet bioprinting. (G) Continuous inkjet. (H) Suspended bioprinting. (I) Selective laser sintering. Created with Biorender [û, NP. (2025). https://BioRender.com/9qrb2ez.

robust, porous scaffolds, as shown in Figure 2I—further expand the design space.

The selection of 3D bioprinting modalities requires meticulous evaluation of factors including cell viability, structural complexity, and industrial scalability. Table 1 summarizes critical parameters for each modality, highlighting their proficiency in constructing multi-scale toxicological models, spanning from micro-level precision to macro-level biomimicry.

3.2. Design of bioinks: natural and synthetic materials

In the realm of bioprinting technology, the choice of bioink—the printing material—is crucial for the successful construction of target structures. Commonly used bioinks primarily consist of natural and synthetic polymers, each possessing distinct advantages and limitations. Synthetic materials excel in mechanical properties, rendering them suitable for fabricating structures where lower biological affinity is acceptable. Conversely, natural materials offer superior biocompatibility and bioactivity but often exhibit weaker mechanical performance, making them well-suited for mimicking native tissues. Therefore, the development and selection of appropriate bioinks are crucial for achieving the ultimate goals of bioprinting.[94]

3.2.1. Natural materials

Natural bioinks derive from biodegradable polymers that hydrolyze or undergo enzymatic degradation *in vivo*, yielding biocompatible byproducts. They are broadly classified as animal-derived or non-animal-derived materials.[95] Among animal-derived polymers, collagen and its thermo-responsive derivative gelatin excel at recapitulating native ECM architecture. However, gelatin's slow, temperature-dependent gelation compromises printing fidelity; methacrylation overcomes this by enabling rapid, tunable ultraviolet-mediated crosslinking and adjustable stiffness.[96] Composite formulations—such as gelatin–alginate blends—have demonstrated enhanced mechanical integrity and cell compatibility for soft-tissue constructs.[97] Non-animal polysaccharides like alginate and hyaluronic acid offer mild ionic or photo-crosslinking, customizable mechanics, and minimal immunogenicity. Alginate rapidly gels in divalent-cation baths (e.g., Ca^{2+}), supporting modular constructs and even laser-induced bioprinting with high cell viability.[98] Silk-based inks—from fibroin or recombinant spider silk—provide superior tensile strength and biocompatibility,[99] though natural spider silk's scalability is limited.[100,101] Recombinant variants and silk-like polypeptides now enable tunable hydrogels and porous scaffolds for diverse tissue engineering applications.[99] dECM bioinks preserve organ-specific biochemical cues (collagens, glycosaminoglycans, laminin) that direct cell phenotype and function.[102,103] For instance, cardiac and cartilage dECM enhance cardiomyocyte maturation and upregulate *SOX9*/*COL2A1* expression, respectively.[103] Yet, complex decellularization, variable gelation kinetics, and insufficient native mechanics often necessitate chemical crosslinkers or synthetic blends to balance printability with physiological performance.[102] In summary, natural materials are highly valued in bioprinting for their excellent biocompatibility and bioactivity. However, their mechanical limitations often require reinforcement through composite formulations. By carefully selecting and modifying natural materials, their potential applications in bioprinting can be substantially expanded.

3.2.2. Synthetic materials

Synthetic polymers have precise control over mechanical properties, degradation rates, and batch-to-batch consistency, making them staples in bioprinting. Polyethylene glycol hydrogels are Food and Drug Administration-approved, highly hydrophilic, and resistant to protein fouling. Low-molecular-weight

Table 1. Overview of common bioprinting techniques

Method	Resolution (μm)	Viscosity (mPa·s)	Cell viability	Build speed	Applications
Extrusion-based bioprinting	100	$30–6 \times 10^7$	50–90%	Slow	Construction of tissue-engineered scaffolds and soft tissue models[76–79]
Stereolithography	50	No limitation	85–95%	Fast	Suitable for fabricating high-precision tissue-engineered scaffolds[77,80–82]
Digital light processing	10	Low	85–95%	Fast	Preparation of drug delivery systems and tissue models[81,83–86]
Inkjet bioprinting	50	3–30	80–90%	Fast	Construction of tissue-engineered scaffolds and drug-screening models[84,87,88]
Laser-assisted bioprinting	10	1–300	~90%	Medium	High-precision cell patterning and tissue-engineered scaffold construction[75,77,89–91]
Selective laser sintering	50	Not applicable	Not applicable	Medium	Fabrication of hard tissue models[83,92,93]

polyethylene glycol (<50 kDa) is metabolizable, and its thermal properties permit customizable stiffness and melting behavior.[99,104–106] Polyvinyl alcohol hydrogels, formed via non-toxic freeze–thaw cycles, deliver excellent transparency, biocompatibility, and enhanced mechanical strength without chemical crosslinkers.[99,107] Poly(lactic-co-glycolic acid)—a lactic/glycolic acid copolymer—degrades into endogenous metabolites, but its hydrophobicity and poor cell adhesion often require surface treatments to improve cell–matrix interactions.[108,109] Polycaprolactone offers robust mechanical strength and biodegradability, making it ideal for load-bearing or vascular scaffolds; functionalization and composite strategies further fine-tune its properties for specific tissue targets.[110–112] Thermo-responsive polymers such as poly(N-isopropylacrylamide) and Pluronic enable temperature-controlled gelation. Poly(N-isopropylacrylamide) transitions at ~37°C but lacks innate biodegradability and adhesion, while Pluronic serves as a sacrificial support due to its reversible gelation, though it demands acrylation or blending to sustain cell viability over time.[113,114] Emerging candidates like polyvinylpyrrolidone have shown promise as bioinks at 0–3% w/v, enhancing printability and uniform cell distribution in preliminary studies.[115] In summary, synthetic materials are highly valued in bioprinting for their superior mechanical properties and tunable degradation rates. However, their limited biocompatibility and cell adhesion necessitate optimization via surface modifications or composite strategies. By carefully selecting and modifying synthetic materials, their potential applications in bioprinting can be substantially expanded.

Natural and synthetic materials both possess unique advantages and limitations. In practical applications, a combination of both is often employed to develop superior composite bioinks that fulfill the diverse requirements of tissue engineering and regenerative medicine. Schematic diagrams of common natural materials in 3D printing and molecular structure diagrams of synthetic materials are shown in Figure 3.

3.3. Construction and integrated applications of *in vitro* models using three-dimensional bioprinting

Three-dimensional bioprinting technology, with its exceptional spatial precision, has shown significant promise in advancing *in vitro* toxicological research by providing innovative methodologies for constructing multi-layered

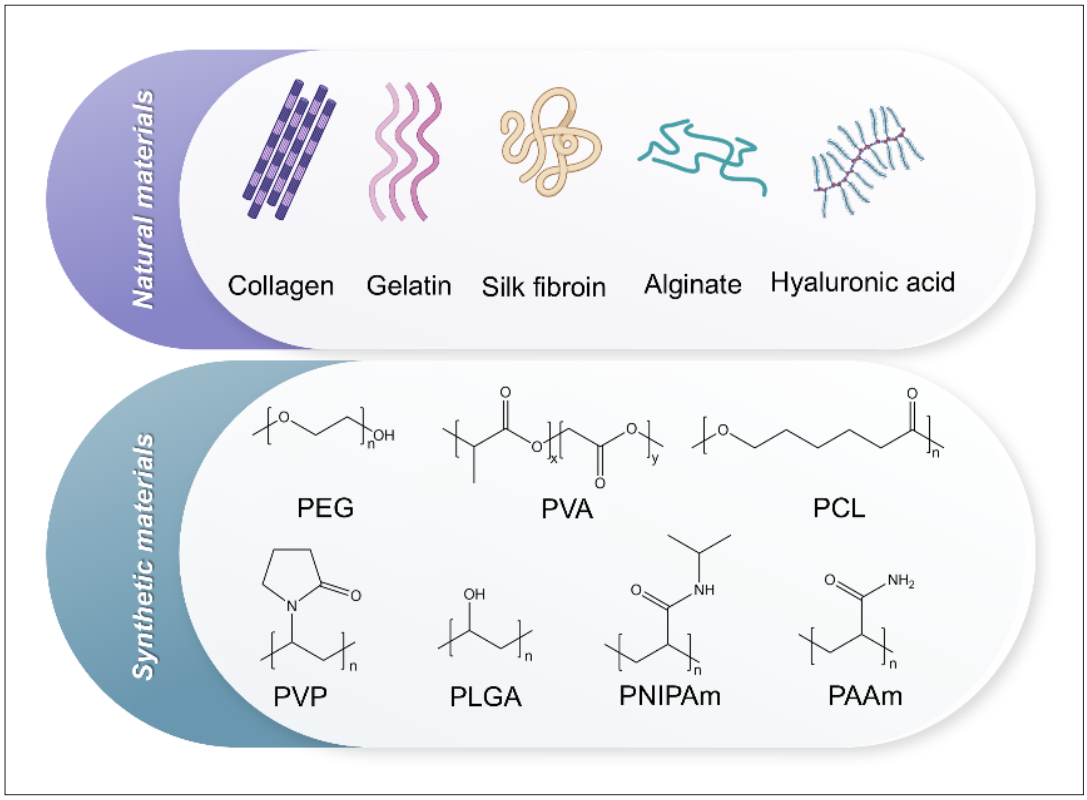

Figure 3. Schematic diagram of natural and synthetic materials commonly used in three-dimensional printing. Partially created with Biorender [û, NP. (2025). https://BioRender.com/3ko1ayt. Abbreviations: PAAm, propylacrylamide; PCL, polycaprolactone; PEG, polyethylene glycol; PLGA, poly(lactic-co-glycolic acid); PNIPAm, poly(N-isopropylacrylamide); PVA, polyvinyl alcohol; PVP, polyvinylpyrrolidone.

models.[116,117] Based on the target of the printing process, the applications of 3D bioprinting are broadly classified into the following two primary approaches: direct printing and indirect printing. Direct printing primarily focuses on the fabrication of tissue and organ models, facilitating the precise replication of human anatomical structures. These models act as indispensable tools for surgical planning, medical education, and regenerative medicine studies. By closely mimicking native tissue architecture, direct printing offers a reliable framework for investigating physiological processes and devising therapeutic interventions.[118] Indirect printing focuses on the development of complex systems, including organ-on-a-chip platforms and sensor-integrated devices. Organ-on-a-chip technology combines microfluidics and biosensors to simulate the physiological functions of human organs, providing a versatile framework for drug screening and disease modeling.[119] These chips allow high-throughput experimentation and predictive assessments, revolutionizing toxicological research.[120] Sensor-integrated platforms leverage embedded electronic components to facilitate real-time observation and analysis of biological processes.[121] These systems provide efficient and accurate tools for biomedical and toxicological research, thereby enhancing the accuracy of experimental processes and the reliability of data. Table 2 summarizes representative applications of 3D bioprinting technologies in tissue modeling, organ-on-a-chip fabrication, and biosensor development, highlighting their adaptability and transformative effects across various disciplines.

3.3.1. Biomimetic construction of tissue-specific models

The construction of tissue-specific models requires the precise replication of critical elements of native tissues, such as ECM composition and mechanical properties.[136] By integrating 3D bioprinting technology with biomaterial processing techniques in tissue engineering, 3D bioprinting enables the rapid fabrication of tissue structures with precise spatial arrangements, thus facilitating the development of physiologically relevant disease models.[137] These models enable detailed analyses of inflammatory responses and immune cell interactions, while offering distinct advantages for studying diseases such as inflammatory bowel disease, Crohn's disease, and colitis. They provide an essential platform for evaluating novel anti-inflammatory therapies.

Almutary *et al.*[138] used 3D bioprinting to create a colitis model integrating Caco-2 and HT-29 cells. Compared to 2D cultures, the 3D model better mimicked intestinal structure and enhanced barrier function. It also verified nanocarrier-based drugs' effectiveness in maintaining intestinal barrier integrity, showing 3D bioprinting's advantages in disease-model construction and drug development. Moreover, Kim *et al.*[139] presented a 3D cell-printing-based skin model for type 2 diabetes patients. Utilizing a hybrid printing platform combining drop-on-demand and extrusion modules, they fabricated a multilayered skin construct that reproduces hallmark diabetic features—insulin resistance, adipocyte hypertrophy, chronic inflammation, and microvascular dysfunction. This innovative *in vitro* model offers a powerful tool for investigating diabetes-related skin pathophysiology and testing topical therapeutics.

Beyond applications in inflammatory disorders, 3D bioprinting has been leveraged to engineer tumor models with remarkable fidelity. By precisely reproducing the complex architecture and cellular heterogeneity of neoplastic tissue, these platforms enable the study of tumor growth, invasion, and metastatic dissemination under physiologically relevant conditions. For instance, Vázquez-Aristizabal *et al.*[140] developed a dECM-based, 3D-printed melanoma model that faithfully mimics the cutaneous microenvironment and malignant phenotype. Their strategy involved formulating a biocompatible "bioink" comprising epidermal, basement membrane, and dermal components, then employing confocal microscopy and surface-enhanced Raman scattering mapping to monitor cell behavior. This system successfully emulated melanoma cell invasion, providing a novel *in vitro* platform for elucidating metastatic mechanisms, as shown in Figure 4A.

The application of 3D bioprinting in toxicological testing also demonstrates substantial potential. Unlike conventional 2D cell cultures, 3D bioprinting offers a novel method for toxicity assessment by simulating more realistic tissue structures, allowing for precise analyses of long-term effects and bioaccumulation of toxic substances. This technology not only facilitates the construction of intricate 3D structures, such as vascularized tissues and neural tissues, but also achieves a degree of precision and complexity unattainable through traditional tissue engineering approaches, as shown in Figure 7.

Additionally, 3D bioprinting is characterized by its high resolution and rapid manufacturing capabilities, allowing for the rapid production of biological tissues or organs while maintaining high cell viability. Another notable feature of 3D bioprinting is its extensive selection of bioink materials, which can be optimized and tailored to fulfill the specific requirements of various tissue types, further expanding its applications in tissue engineering. In cardiovascular tissue engineering, microchannel-based 3D bioprinting has been employed to fabricate novel cardiac patches that promote cell alignment, thereby minimizing the cell requirements for cardiac regeneration

Table 2. Applications of common three-dimensional printing techniques in tissue modeling, organ-on-a-chip fabrication, and biosensor production

Method	Target	Materials	Cell types	Applications
EBB	Three-dimensional scaffolds for bone tissue engineering	Hyaluronic acid; chitosan	MG63	Bone defect repair and bone tissue regeneration research[122]
	In vitro air-blood barrier model	Matrigel	A549; EA.hy926	*In vitro* models for lung disease research and drug testing[17]
	Printable POC biosensors	Organoxilane polymer, AuNR, protein A, IgG	—	Manufacturing stable biosensors for early disease diagnosis[79]
	Human skin tissue	Collagen	HaCaT; HFF-1	*In vitro* models for skin grafts and wound healing research[123]
Inkjet	Multi-cell heterogeneous tissue constructs	SA; collagen	hAFSCs; dSMCs; bECs	Constructing complex tissue models with multiple cell types for tissue engineering research[124]
	Liver-on-a-chip	SA	HepG2; U251	Drug metabolism and diffusion experiments to imitate *in vivo* situations[79]
	Hybrid nasal cartilage with electronic olfaction	GelMA; PEGDMA	Chondrocytes; ADSCs; HUVECs	Electronic olfaction[125]
SLA	Cell loading model	PEGDA; GelMA	NIH 3T3	Cell patterning in tissue engineering and bioengineering[126]
	Vascularized bonemimetic hydrogel	Gelatin; GelMA	HUVEC; C3H10T1/2	Bone tissue engineering, promoting osteogenesis and angiogenesis[127]
	Hydrogel scaffolds	PAA	—	Develop an ultrasensitive fiber-optic pH sensor[128]
	Engineered biofilms with bacteria	PEGDa bioresins	*Escherichia coli*; *Caulobacter crescentus*	Uranium element detection[82]
LAB	Microneedles	PMMA	—	Transdermal delivery of chemotherapeutic drugs via microneedles[129]
	Skin-on-a-chip	Collagen	NIH3T3; HaCaT	Constructing skin-like organs with functions[91]
DLP	Human iPSC-derived hepatic model	GelMA; GMHA	hiPSC-HPCs; HUVECs;vADSCs	Drug screening and disease modeling[86]
	Liver lobule microtissue biosensor	HAMA hydrogel, MWCNTs	HepG2	Aflatoxin B1 detection[130]
	Lung-on-a-chip	Resin (BV-007)	Calu-3	Respiratory toxicological testing and pulmonary drug delivery studies[131]
	Patterned cell-laden heart and liver tissue constructs	GelMA; HdECM	hiPSC-CMs; hiPSC-Heps	Serve as potential physiologically-relevant living human tissue platforms[132]
SLS	Three-dimensional nanocomposite scaffolds for bone tissue engineering	Ca-P/PHBV; CHAp/PLLA	SaOS-2	Bone tissue engineering, constructing biomimetic bone scaffolds[93]
	Cell density sensor	Metallic powder; polyamide; PVC	—	Monitoring cell density[133]
Suspended bioprinting	Multiple-layered vascular models	VdECM; Pluronic F127	HUVECs; HCASMCs	*In vitro* modeling of the initiation of arterial disorders[134]
	Full-size model of the heart	Gelatin microparticles; SA	—	Surgical simulation and training[135]

Abbreviations: ADSCs, adipose-derived stem cells; AuNR, gold nanorods; bECs, bovine aortic endothelial cells; Ca-P/PHBV, calcium phosphate/poly(hydroxybutyrate-co-hydroxyvalerate); CHAp/PLLA, carbonated hydroxyapatite/poly(L-lactic acid); DLP, digital light processing; dSMCs, canine smooth muscle cells; *E. coli*, *Escherichia coli*; EBB, extrusion-based bioprinting; GelMA, gelatin methacrylate; GMHA, glycidyl methacrylate hyaluronic acid; hAFSCs, human amniotic fluid-derived stem cells; HAMA, methylacylated hyaluronic acid; HCASMCs, human coronary artery smooth muscle cells; HdECM, heart decellularized extracellular matrix; hiPSC-Heps, human induced pluripotent stem cell-derived hepatocytes; hiPSC-CMs, human induced pluripotent stem cell-derived cardiomyocytes; hiPSC-HPCs, human induced pluripotent stem cell-derived hepatic progenitor cells; HUVECs, human umbilical vein endothelial cells; IgG, immunoglobulin G; LAB, laser-assisted bioprinting; MWCNTs, multi-walled carbon nanotubes; PAA, poly(acrylic acid); PEGDA, polyethylene glycol diacrylate; PEGDMA, polyethylene glycol dimethacrylate; PMMA, polymethylmethacrylate; PVC, polyvinyl chloride; SA, sodium alginate; SLA, stereolithography; SLS, selective laser sintering; VdECM, vascular decellularized extracellular matrix.

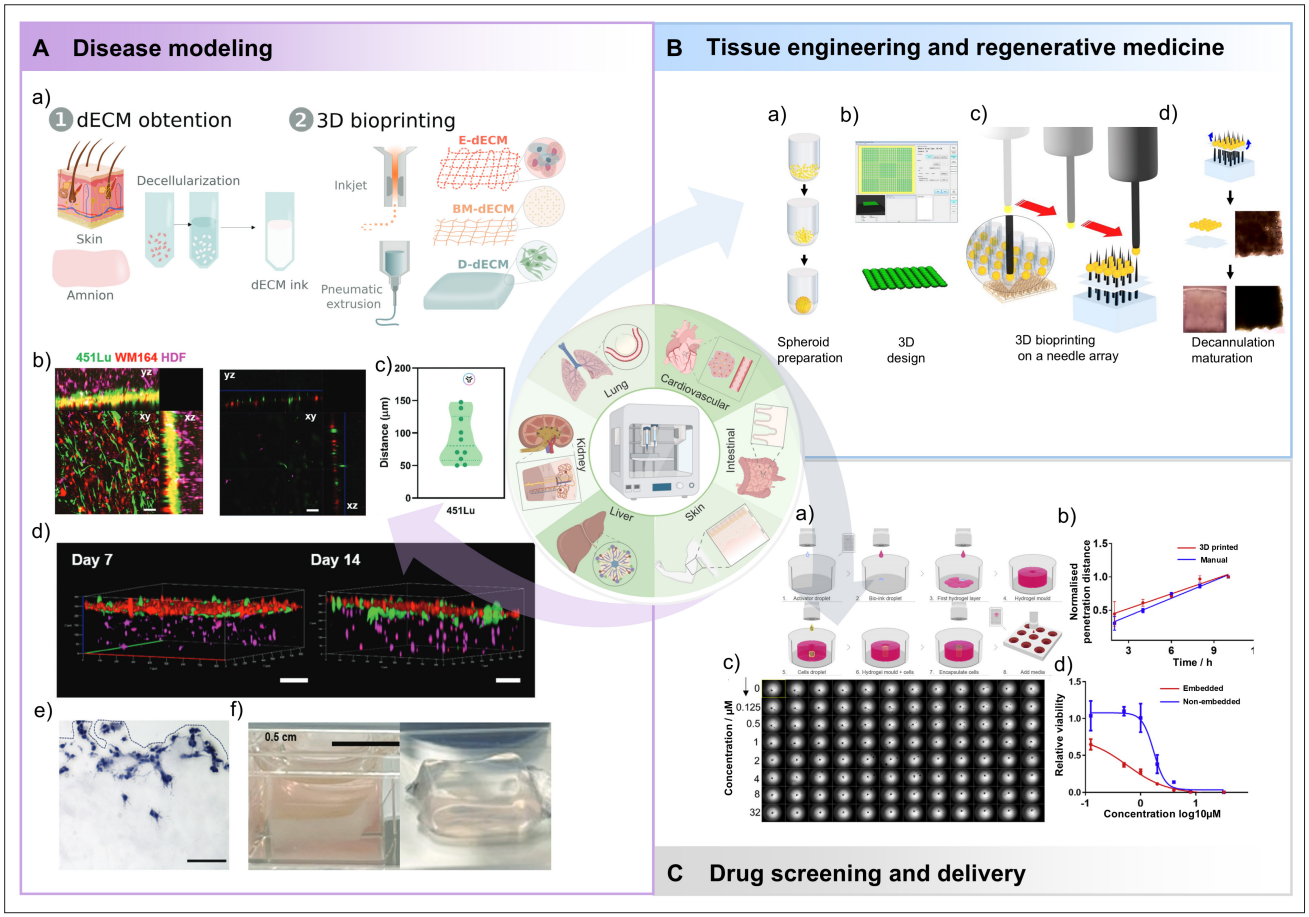

Figure 4. Biomimetic construction of tissue-specific models. (A) Three-dimensional (3D)-printed melanoma invasion model. (a) Workflow for biomaterial formulation and 3D printing of the layered melanoma–dermis construct. (b) Orthogonal maximum-intensity projection showing 451Lu melanoma cells (green) invading the human dermal fibroblast (HDF)-laden dermis (magenta) after 14 days (left), and single-plane detail of a protrusive metastatic cell (right). Scale bar: 100 µm. (c) Measured invasion distances of 451Lu cells into the dermal decellularized extracellular matrix (dECM). (d) 3D reconstructions of the bioprinted model at Days 7 and 14. Scale bars: 150 µm. (e) Hematoxylin and eosin staining of melanoma cells penetrating the dermal matrix. Scale bar: 100 µm. (f) Macroscopic appearance of the layered model at Days 14 and 21 in culture. Scale bar: 0.5 cm. Adapted with permission from Vázquez-Aristizabal *et al.*[140] (B) Schematic of a biomaterial-free 3D bioprinting approach for cardiac tissues. (a) Cardiospheres are formed by aggregating cells in ultra-low attachment 96-well plates. (b) A desired 3D architecture is designed using computer-assisted design software. (c) Cardiospheres are picked up individually using vacuum suction and positioned on a microneedle array by the 3D bioprinter. (d) After fusion, the tissue is removed and cultured further to allow self-healing of needle-induced voids. Adapted with permission from Ong *et al.*[143] (C) Drug penetration and viability in bioprinted spheroids. (a) Diagram of the bioprinting workflow for embedding spheroids in hydrogel. (b) Doxorubicin penetration depth over 10 h in bioprinted *versus* manually formed spheroids (n = 2, three spheroids per group). (c) Operetta image of a full 96-well plate containing bioprinted spheroids prior to treatment. (d) Dose–response curves for embedded and non-embedded spheroids after eight doxorubicin concentrations (n = 2, six spheroids per condition). Adapted with permission from Utama *et al.*[147] Partially created with Biorender [ù, NP (2025). https://BioRender.com/qvrla5y.

and fibrosis prevention.[141] This technology has also been used to produce hydrogel patches for treating myocardial infarction patients.[142] Furthermore, multicellular spheroids have been printed onto needle arrays to form tubular cardiac tissues to evaluate therapeutic efficacy, contractile force, and beating rhythms,[143] as shown in Figure 4B. Scaffold-free bioprinting techniques have also garnered attention for their capacity to fabricate cardiac scaffolds without the use of biomaterials.[144,145]

In pharmaceuticals, the applications of 3D bioprinting are primarily centered on drug screening and delivery systems. By fabricating structures that mimic the spatial and chemical attributes of native tissues, 3D bioprinting supports drug screening and facilitates the development of both simple and complex drug delivery systems. As early as 2003, Mironov *et al.*[146] proposed that perfused and vascularized human tissue or organ structures fabricated through 3D bioprinting could serve as efficient systems for drug screening. Since then, researchers have explored the use of 3D bioprinting to construct biomimetic 3D *in vitro* models that replicate native tissues or organs, allowing for more precise drug screening.

Three-dimensional bioprinting also holds great promise for the development of high-throughput, precision drug-screening assays. Utama *et al.*[147] engineered a bioprinting platform capable of fine-tuning cell number, spheroid diameter, and hydrogel "cup" geometry to mass-produce embedded multicellular spheroids, as shown in Figure 4C. Impressively, this method maintained over 98% cell viability while yielding spheroids whose proliferation, apoptotic profiles, and stem-cell marker expression closely matched those of manually assembled controls. Notably, the model exhibited a size-dependent drug response: larger spheroids, owing to diffusion gradients, displayed significantly elevated half-maximal inhibitory concentration values, and variations in cup dimensions directly influenced pharmacodynamic readouts. These findings offer new insights into modeling solid-tumor chemoresistance with high fidelity. Concurrently, Matsusaki *et al.*[148] utilized inkjet bioprinting to fabricate layered 3D liver-tissue microarrays featuring endothelial-hepatocyte heterotypic architecture; their automated workflow provides a scalable paradigm for preclinical toxicology screening. Although current 3D constructs remain imperfect in replicating native tissue diffusion dynamics, vascularization, and chemical gradient formation, ongoing optimization of physicochemical parameters and microenvironmental design is poised to surmount these limitations and yield more clinically relevant *in vitro* drug-screening platforms.[83]

To enhance the simulation of *in vivo* physiological environments, researchers have employed microfluidic networks to maintain and connect microtissues and organ units, thereby enabling the development of "organ-on-a-chip" devices. By incorporating microfluidic perfusion channels, these chips can recreate vascular systems, dynamic cellular culture environments incorporating mechanical and chemical stimuli, and nutrient and oxygen exchange under controlled concentration gradients. The specific features and applications of organ-on-a-chip technology will be discussed in the following section.

3.3.2. Functional integration of organ-on-a-chip technology

The application of 3D bioprinting in advanced organ-on-a-chip devices serves as a potent tool for improving the biological relevance of disease models and drug testing platforms. Recent advancements in organ-on-a-chip research, including the integration of bioprinting technologies, have effectively addressed numerous limitations inherent to traditional microfluidic chip fabrication. Conventional methods, such as lamination and molding, are labor-intensive, expensive, and ill-suited for fabricating intricate 3D structures.[149,150] Additionally, cell seeding in microchannels typically relies on manual operations or syringe pumps, which are cumbersome, inefficient, and reliant on intricate fluidic connections. Furthermore, most biomimetic organ chips fail to replicate the 3D growth environments of native tissues or support the construction of heterogeneous tissue structures, impeding accurate simulation of dynamic blood flow and heterogeneous cellular distributions at the microscale level in organ systems.[151]

The rapid development of 3D bioprinting, leveraging versatile bioink materials, diverse printing techniques, and flexible 3D design capabilities, has proven to be a transformative solution to overcome these challenges.[16] This technology enables the fabrication of intricate 3D structures and the seamless integration of biomimetic structural and functional units, offering a more streamlined method for fabricating complex tissue and organ models.[16] To date, 3D bioprinting has found successful application in the fabrication and functional modeling of organ-on-a-chip systems for various organs, including the heart, liver, kidney, tumor tissues, and nervous system.[19,152–154]

In the context of organ-on-a-chip fabrication, 3D bioprinting commonly employs the following two methodological approaches: the two-step method and the one-step method. The former entails the separate fabrication of microfluidic chips, followed by the printing of biological tissues or micro-organoids onto the pre-assembled chips.[155,156] While this approach utilizes 3D bioprinting for certain processes, it is labor-intensive and exhibits limited reproducibility. Conversely, the one-step method integrates the entire fabrication process, simultaneously printing both biomimetic structural units and biological functional units, providing a more integrated and efficient solution.[157] Widely utilized bioprinting techniques for organ-on-a-chip systems encompass inkjet printing, extrusion-based printing, and photocuring-based printing.

In the realm of organ-on-chip engineering, 3D printing technologies have demonstrated exceptional versatility and manufacturability, enabling the precise reconstruction of complex biological interfaces. In the context of renal physiology and functional assessment, Lin *et al.*[158] optimized ECM composition and fugitive-ink formulations to co-print vascularized proximal tubules within a highly permeable hydrogel matrix, establishing a closed-loop perfusion circuit. This platform not only facilitated functional co-culture of proximal-tubule epithelial and endothelial cells but also quantified active albumin/glucose reabsorption and recapitulated high-glucose-induced endothelial injury, thereby offering a high-fidelity system for renal physiology studies and nephrotoxicity assessment. For liver function modeling and drug testing applications, Fritschen *et al.*[159] developed an innovative, high-throughput 3D bioprinting platform that integrates drop-on-demand bioprinting

with robotic handling, as shown in Figure 5A. This system employs a sealed, 3D-printed microfluidic chip featuring a central tissue chamber flanked by arterio-venous mimic channels, laying the groundwork for microvascular network self-assembly. By utilizing agarose and fibrinogen bioinks, they successfully constructed a multicellular, vascularized hepatocellular carcinoma model. The platform's automation dramatically enhances both efficiency and reproducibility, and in a HepG2 model, it demonstrated stable microvascular network formation,

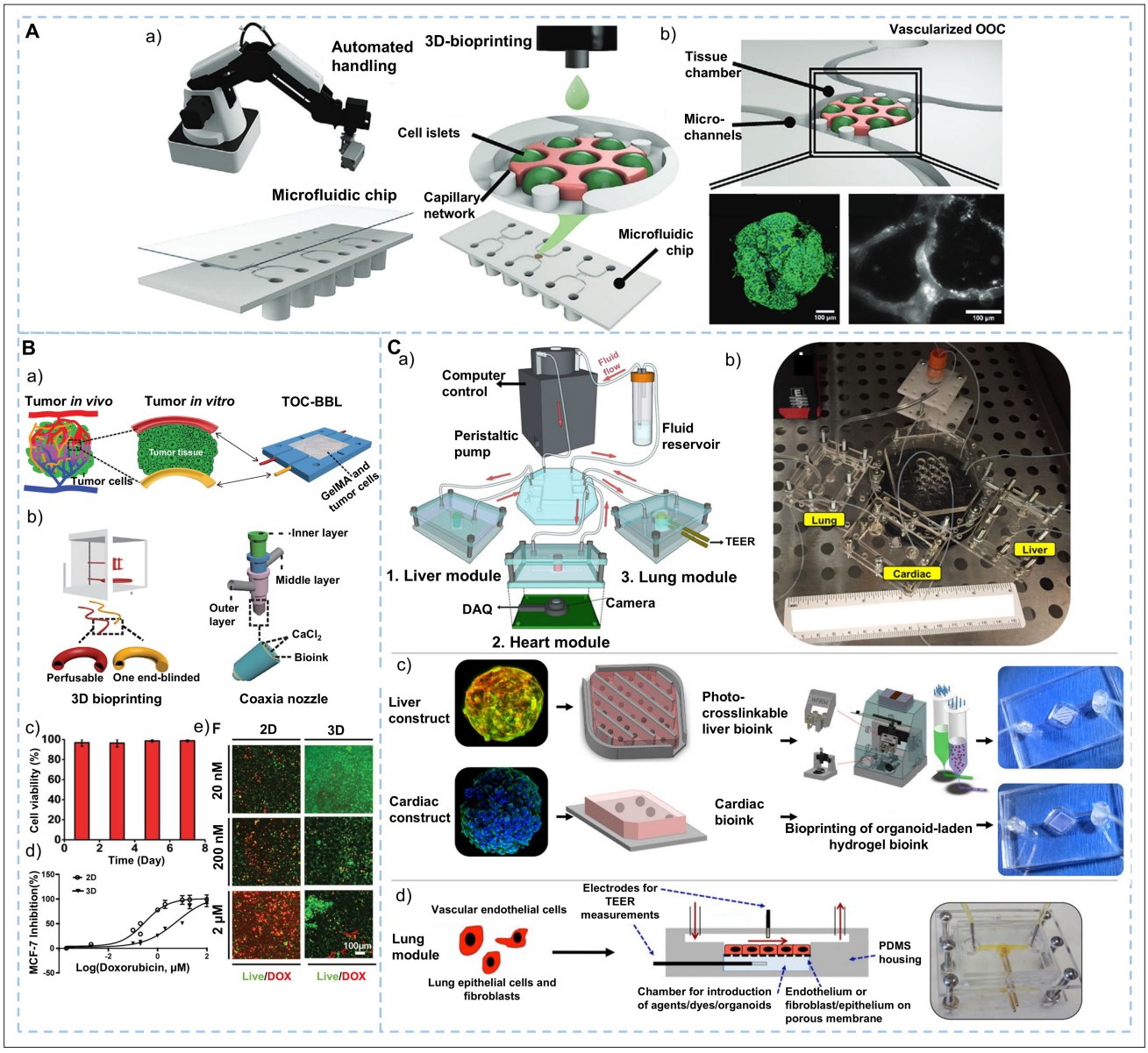

Figure 5. Applications of three-dimensional (3D) printing in organ-on-a-chip design. (A) Schematic of the automated fabrication workflow for vascularized organs-on-chips (OOCs). (a) A robotic platform precisely loads and unloads custom microfluidic chips during the pre- and post-processing stages of 3D bioprinting. (b) Within the chip's tissue chamber, printed HepG2 cells proliferate into spheroidal aggregates as a perfusable microvascular network self-assembles over the culture period. Adapted with permission from Fritschen *et al.*[159] (B) Tumor-on-a-chip with bioprinted blood-lymphatic pair (TOC-BBL). (a) Schematic of TOC-BBL featuring adjacent bioprinted blood and lymphatic vessels. (b) Overview of the custom 3D-printing setup and fabrication workflow for TOC-BBL. (c) Viability quantification of cells within the TOC-BBL platform. (d) Doxorubicin (DOX) dose-response curves for MCF-7 cells in two-dimensional culture *versus* 3D TOC-BBL. (e) Fluorescence micrographs showing MCF-7 viability under increasing DOX concentrations ($p < 0.01$). Scale bar: 100 μm. Adapted with permission from Cao *et al.*[162] Copyright © 2019 Wiley-VCH. (C) Integration of multiple tissues in a modular organ-on-a-chip platform. (a & b) Diagrams and images of the plug-and-play system enabling parallel culture of three tissue types via interconnected microreactors. (c) Liver and cardiac modules are generated by printing spheroids within custom bioinks. (d) Lung models are developed by layering cells over porous membranes, with transendothelial electrical resistance (TEER) sensors integrated for barrier integrity monitoring. Adapted with permission from Skardal *et al.*[165]

robust cell proliferation, and sustained albumin secretion, underscoring its promise for scalable drug screening and toxicity assays.

Cardiovascular disease modeling represents another pivotal application of 3D-printed organ chips. Zhang *et al.*[160] employed microfabrication-enabled 3D printing of GelMA to create a thrombus-on-a-chip, integrating fibroblasts and endothelialized microchannels to simulate thrombosis and fibrotic progression under dynamic flow. Abudupataer *et al.*[161] developed a photocurable bioprinted vascular model containing smooth muscle and endothelial cells, establishing a dynamically perfused vessel construct for vascular disease research. Tumor microenvironment models have likewise advanced beyond single-vessel systems. Cao *et al.*[162] used multi-material bioprinting to generate a tumor-on-a-chip with bioprinted blood-lymphatic pair chip incorporating both perfusable blood vessels and blind-ended lymphatics, modulating GelMA matrix permeability to recapitulate differential drug diffusion kinetics across blood and lymphatic compartments, as shown in Figure 5B. Xie *et al.*[163] further demonstrated electrohydrodynamic jetting to array tumor-cell-GelMA droplets, creating a chip that balances high viability with compatibility for high-throughput screening. Additionally, Johnson *et al.*[164] printed polycaprolactone microchannels via extrusion to fabricate a neural connectivity platform, highlighting 3D printing's customizability in neuro-organ-on-chip design. Collectively, these advances validate the unique strengths of 3D bioprinting for multi-tissue integration and dynamic microenvironment construction, and—through precise control of bioink rheology, spatial resolution, and mechanical properties—significantly enhance the simulation of key pharmacodynamic parameters such as drug penetration and metabolic response. Looking ahead, the fusion of multi-modal bio-fabrication techniques with enhanced vascular network maturation promises to overcome current challenges in long-term culture stability and tissue complexity.

To simulate interactions among multiple organs and better reflect human physiological and pathological processes, Skardal *et al.*[165] constructed a three-organ chip system comprising lung, liver, and heart tissues using 3D extrusion bioprinting, as shown in Figure 5C. By integrating organ-specific bioinks and customized fluidic devices, this system highlighted the utility of multi-organ combinations in evaluating drug efficacy and side effects. The exploration of novel bioprinting techniques continues to address the diverse demands of organ-on-a-chip technology. Elezoglou *et al.*[166] employed laser-induced forward transfer to deposit lung cancer cells onto organ chips, facilitating the study of cancer cell migration, with high-speed camera systems incorporated for real-time observation of bioink ejection mechanisms. Bowser *et al.*[167] used magnetic bioprinting to fabricate central nervous system chips, employing magnetic NPs to create spinal cord spheroids precisely positioned within hydrogel structures. Combined with digital projection lithography, this method enhances structural uniformity and facilitates long-distance 3D neural projections.

These studies highlight the extensive application potential of 3D bioprinting in organ-on-a-chip technology, ranging from single-tissue models to multi-organ systems. 3D bioprinting offers powerful tools for disease research, drug development, and personalized medicine, surpassing the limitations of traditional fabrication methods and fostering innovation in the field.

3.3.3. Customized development of biosensors

The relationship between 3D bioprinting and sensor platforms is characterized by both intricacy and versatility. By enabling the creation of sensors with complex geometries, controlled microstructures, and tailored material combinations, 3D bioprinting facilitates the development of devices that more accurately replicate the characteristics of biological tissues.[168] This capability supports miniaturization, customization, and enhanced flexibility of sensors, thus enhancing their performance and broadening their scope of applications.[168] Widely utilized 3D printing techniques in this field include fused deposition modeling, inkjet printing, direct extrusion, and stereolithography, each facilitating the rapid and cost-efficient production of advanced biomedical sensors.

Regarding inkjet printing, Cagnani *et al.*[169] developed a roll-to-roll inkjet-printed biosensor by precisely depositing tyrosinase-based bioink onto screen-printed carbon electrodes via a slot-die coating process. This biosensor achieved successful dopamine detection with an enzyme activity retention rate exceeding 98%, offering a viable pathway for the scalable, low-cost production of disposable diagnostic devices. Notably, Wang *et al.*[170] introduced an electric-field-driven microscale 3D printing technique capable of finely shaping polydimethylsiloxane doped with multiwalled carbon nanotubes composite microchannels, as shown in Figure 6A. The resulting flexible sensor demonstrated 84% optical transparency and a strain gauge factor as high as 1500. With its exceptional performance in monitoring human motion, this sensor exhibits clear advantages in wearable healthcare applications, enabling comprehensive detection from millimeter-scale joint movement to micron-scale facial expressions.

In the domain of laser fabrication, Wu *et al.*[171] developed a laser direct-write graphene ammonia sensor featuring a

3D porous architecture and an integrated heater design. This innovation reduced response and recovery times to 214 and 222 s, respectively, and achieved a sensitivity of 0.087% 1/ppm. Its dual-mode heating mechanism enhanced gas desorption efficiency, laying the groundwork for the development of wearable respiratory monitoring devices, as shown in Figure 6B. Expanding the frontier of laser technology, Hecht *et al.*[172] employed bubble-assisted laser-induced forward transfer to achieve submicron-scale patterning of polyimide-based bioinks on nitrocellulose substrates, as shown in Figure 6C. This approach enabled the fabrication of a multichannel C-reactive protein detection system while maintaining material integrity under high-energy laser exposure, thus offering a robust manufacturing route for point-of-care diagnostic devices.

Photopolymerization-based 3D printing, known for its high-resolution microstructural fabrication, has opened new avenues in biosensing applications. Cao *et al.*[173] employed stereolithography to construct a paper-based microfluidic screen-printed electrode integrated with reduced graphene oxide-tetraethylene pentamine/Prussian blue composite materials, achieving a glucose detection limit of 25 μM, which is comparable to commercial glucose meters. This integrated approach, which combines microfluidic channels with electrochemical sensing units, significantly enhances detection efficiency and supports personalized diabetes management. Simultaneously, extrusion-based 3D printing has achieved key breakthroughs in multifunctional sensor integration due to its superior material compatibility. Marzo *et al.*[174]

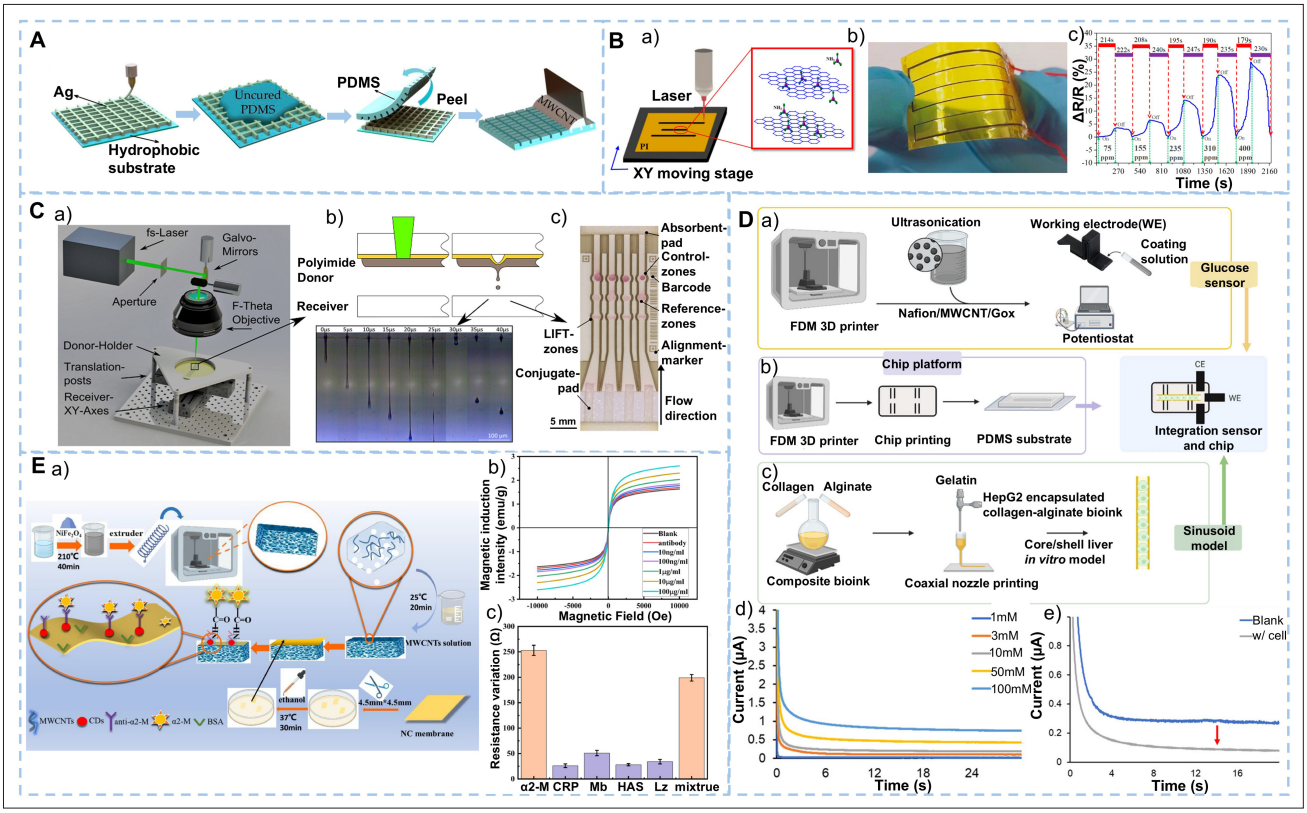

Figure 6. Applications of three-dimensional (3D) printing in biosensor construction. (A) Fabrication of a flexible strain sensor. Process schematic of a flexible strain sensor with embedded multiwalled carbon nanotubes composite microchannel (MWCNT) network. Adapted with permission from Wang *et al.*[170] (B) Laser direct writing for flexible ammonia gas sensor. (a) Schematic of the laser direct writing process. (b) Photograph of a flexible zigzag sensor pattern fabricated via laser writing. (c) Real-time response/recovery curves to ammonia concentrations from 75 to 400 ppm. Adapted with permission from Wu *et al.*[171] (C) Blister-actuated laser-induced forward transfer printing for multifunctional paper biosensors. (a) Overview of the printing setup with typewriter-like receiver movement. (b) Key parameters and stroboscopic imaging of droplet formation at 2.5 μJ. Scale bar: 100 μm. (c) Prototype of a multichannel lateral flow test fabricated entirely by laser printing. Adapted with permission from Hecht *et al.*[172] (D) 3D-printed glucose sensor and cell-culture assay. (a) Fabrication of carbon black (CB)-polylactic acid (PLA) working electrode and surface coating protocol. (b) Assembly of the PLA chip platform onto glass using polydimethylsiloxane (PDMS). (c) Bioprinted sinusoid-mimetic hydrogel (alginate-collagen). Scale bar: 4.5 mm. (d) Chronoamperometric response of the CB-PLA electrode to glucose (1–100 mM). (e) Glucose measurement in 3D-cultured cells on Day 2. Adapted with permission from Lee *et al.*[175] Copyright © 2023 Wiley-VCH. (E) Electrochemical biosensor for α2-macroglobulin. (a) Schematic of sensor fabrication and anti-α2-macroglobulin modification and detection. (b) Magnetization hysteresis loops for α2-macroglobulin at 10 ng/mL–100 μg/mL. (c) Specificity assay against potential interferents. Adapted with permission from Guo *et al.*[176]

developed an enzymatic graphene-polylactic acid (PLA) electrode by embedding horseradish peroxidase directly into the printed structure, enabling hydrogen peroxide detection down to 11.1 μM. Similarly, Lee *et al.*[175] utilized FDM technology to fabricate a carbon black-PLA three-electrode system, incorporating multiwalled carbon nanotube surface modifications to extend the glucose detection range to 1–100 mM (R^2 = 0.9813). This sensor was seamlessly integrated with a liver-on-chip platform, providing a real-time solution for drug toxicity assessment, as shown in Figure 6D. Guo *et al.*[176] further advanced the field by fabricating nickel ferrite/PLA grid substrates via FDM printing and coupling them with carbon quantum dot-based fluorescent probes to construct a magnetoelastic biosensor, as shown in Figure 6E. This device achieved ultrasensitive detection of α2-macroglobulin at 0.506 ng/mL. The dual-mode magnetic-optical signal conversion mechanism offers an innovative tool for early diagnosis of diabetic nephropathy.

In summary, 3D printing technologies demonstrate substantial potential for advancing the development of biosensors and diagnostic devices. From low-cost, rapidly manufactured bioreactors to highly sensitive biosensors, these innovations can be effectively integrated with printed tissue models and organ-on-a-chip systems to enable real-time monitoring, dynamic regulation, and high-throughput analysis of cellular and tissue functions. The convergence of these technologies augments the biomimicry and applicability of organ-on-a-chip systems while unlocking new opportunities for drug development, disease modeling, and personalized medicine.

4. Applications in organ-specific toxicology

Toxicological testing systems comprise four fundamental domains as follows: drug safety assessment, food contaminant screening, environmental toxicity analysis, and evaluation of the biological effects of nanomaterials. Technological advancements in these areas hold strategic importance for public health safety and sustainable development. In drug development, preclinical models' predictive power is limited, causing around 30% of drug candidates to fail due to uncontrollable toxicity or adverse effects, and resulting in huge annual global economic losses.[177] 2D cell models, lacking the tissue-specific microenvironment—such as the ECM topology and multicellular interaction networks—are inadequate for accurately simulating the dynamic interplay between drug metabolism and toxicity.[47] Consequently, critical toxic phenotypes, including hepatotoxicity and QT interval prolongation, show high false negative rates.[178] Environmental toxicology encounters even more significant challenges. According to the United Nations Environment Programme, over 100,000 new synthetic chemicals are introduced into the ecological cycle annually, yet a mere 0.1% are subject to comprehensive toxicity evaluation.[179] Existing *in vitro* detection technologies are limited by their inability to simulate essential aspects of the air–liquid interface and reconstruct chronic exposure effects.[180] This inability to accurately predict the bioaccumulation and transgenerational toxicity of substances such as particulate matter and persistent organic pollutants presents substantial challenges for ecological risk assessment. In the realm of food safety, foodborne pathogenic toxins (e.g., aflatoxin B1), illegal additives, and microplastic contamination collectively lead to direct global economic losses annually.[181,182] Traditional detection methods, which rely on animal testing coupled with high-performance liquid chromatography, are characterized by low throughput, high costs, and ethical concerns. Nanotoxicology research introduces even greater scientific complexities.[183] They exhibit unique properties, such as surface plasmon resonance and quantum size effects, capable of inducing non-dose-dependent toxicities (e.g., mitochondrial autophagy dysfunction).[184] However, conventional *in vitro* models fail to replicate key features such as tissue penetration and the dynamic interactions between NPs and biological barriers, thereby limiting their effectiveness in accurately predicting nanotoxicological outcomes.[185,186]

Three-dimensional bioprinting technology provides a revolutionary solution to these challenges by enabling the construction of biomimetic structures across multiple scales (resolution of 1–200 μm), regulating dynamic perfusion (shear stress of 0.1–20 dyn/cm^2), and reconstructing heterogeneous microenvironments (co-localization of 3+ cell types).[187,188] This technology has significantly advanced toxicological research across key target organs, including the liver (metabolic toxicity), kidney (excretory toxicity), lungs (inhalation toxicity), cardiovascular system (functional toxicity), intestines (absorption toxicity), and skin (contact toxicity), as shown in Figure 7 and Table 3. This section systematically explores the application of 3D bioprinting in toxicology, highlighting its technical breakthroughs from structural biomimicry to functional integration. Furthermore, clinical relevance validation data are provided to support the scientific rationale for substituting traditional methods with 3D bioprinting approaches. By bridging the gap between *in vitro* models and *in vivo* physiology, 3D bioprinting holds the potential to redefine toxicological testing systems, creating pathways for more accurate, efficient, and ethically sound methodologies.

4.1. Liver toxicology

The liver, as the central organ for xenobiotic metabolism, accounts for over 90% of phase I and II detoxification

Table 3. Application of three-dimensional printing technology in extracorporeal toxicity testing for different organs

Target organ	Printing method	Printing object	Materials	Cell types	Applications
Liver	Continuous deposition microextrusion	3D primary liver tissues	NovoGel1 2.0	**PHH**; **HSCs;** HUVECs	Antibiotic drug toxicity testing[194]
	Direct-write	Liver-on-a-chip platform	GelMA	HepG2; C3A	Drug toxicity assessment of APAP[153]
	Extrusion bioprinting	Hepatic model	SA; Gelatin	hiPSC-Heps	Drug-induced hepatotoxicity evaluation of APAP[195]
	Extrusion bioprinting	Liver lobule microarchitecture	ECM-derived microparticles; BA silk fibroin; gelatin; β-D galactose	HLCs; HUVECs; HHSCs	Hepatotoxicity/non-hepatotoxicity drug toxicity testing[196]
	DLP	Liver lobule microtissue biosensor	HAMA; multi-walled carbon nanotubes	HepG2	The detection of AFB1[130]
	Microextrusion	Xeno-free 3D-bioprinted liver model	Matrigel; SA; human collagen	HuH-7	Toxicity testing of OA[197]
	Electro-assisted bioprinting	Disse space organoids	SA; NC Laminin 511	hPSC-HE; hiPSC-EPCs; LX-2	Toxic mechanisms of MPs and TBBPA in liver tissues[189]
	Magnetic levitation and bioprinting	Mini liver models	Magnetic nanoparticles	Fao	Assessment of the toxicity of nanodiamond[198]
Kidney	Coaxial nozzle extrusion bioprinting	Vas-POAC	Pluronic F127; SA; KdECM	RPTEC; Ges	Evaluation of the cisplatin-induced nephrotoxicity capacity[199]
	Extrusion bioprinting	3D convoluted renal proximal tubules	Fibrinogen; gelatin; Pluronic F127; two-part silicone elastomer	PTECs	Cyclosporine A toxicity testing[19]
Lung	Inkjet bioprinting	3D alveolar barrier	Collagen	HULEC-5a; MRC5; NCI-H1703; NCI-H441	Evaluate the physiological impact of ne dust particles[190]
	Inkjet bioprinting	Lung cancer-on-chip	Nusil medical grade silicone elastomer	NCI-H1437	Physiological monitoring and toxicity assessment of DOX/ docetaxel[200]
	SLA	*In vitro* exposure system	Resin	HBECs	Assessing the effects of cannabis inhalation on the lungs[201]
	Extrusion bioprinting	Organoid-based scaffolds	SA; Matrigel; porcine gelatin	Calu-3	Long-term nanoparticle toxicology investigation[202]
Cardiovascular	Coaxial nozzle extrusion bioprinting	Endothelialized myocardium and heart-on-a-chip	SA; GelMA	HUVECs; hiPSC-CMs	Cardiovascular toxicity evaluation[203]
	Microextrusion bioprinting	Tissue-sensor platform	CB; PCL; soft rubber; PDMS; HdECM	hiPSC-CMs; hCFs	Monitoring of drug-induced cardiotoxicity[191]
	μCOP	Cardiac micro-tissue	GelMA; HAGM	hiPSC-CMs; hCFs	Test the impact of CuO NPs on 3D cardiac micro-tissues[204]
Intestinal	SLA	Intestinal microvillus cell sensor	FCONp; MWCNT-CDH; GelMA	RBL-2H3	The detection of wheat allergen gliadin[205]
	Microextrusion bioprinting	Intestinal barrier models	Collagen	Caco-2; HT-29; HDFn	Studying the permeability and toxicity of ibuprofen[206]
Skin	Extrusion-bioprinting	3D thickness skin tissue model constructs	Novogel 2.0; Fibrinogen	NKTC; NDF; NHEK	Screen topical-use compounds for irritation potential[193]

Abbreviations: 3D, three-dimensional; AFB1, Aflatoxin B1; APAP, acetaminophen; CB, carbon black; CuO, copper oxide; DLP, digital light processing; Fao, rat hepatoma cells; FCONp, flower-like copper oxide nanoparticles; GelMA, gelatin methacrylate; GEs, primary human glomerular endothelial cells; HAGM, hyaluronic acid glycidyl methacrylate; HAMA, methylacylated hyaluronic acid; HBECs, primary human bronchial epithelial cells; HCFs, human cardiac fibroblasts; HDFn, human dermal fibroblasts; HdECM, heart decellularized extracellular matrix; HHSCs, human hepatic stellate cells; hiPSC, human induced pluripotent stem cells; hiPSC-EPCs, endothelial progenitor cells; hiPSC-Heps, human induced pluripotent stem cell-derived hepatocytes; hiPSC-CMs, human induced pluripotent stem cell-derived cardiomyocytes; HLCs, hepatocyte-like cells; HSCs, hepatic stellates; HULEC-5a, lung microvascular endothelial cells; HUVECs, human umbilical vein endothelial cells; KdECM, kidney decellularized extracellular matrix; MPs, microplastics; MWCNT-CDH, multiwalled carbon nanotubes; NDF, neonatal human dermal fibroblast; NHEK, normal human epidermal keratinocytes; NKTC, human primary neonatal keratinocytes; OA, Okadaic acid; PCL, polycaprolactone; PDMS, polydimethylsiloxane; PHH, primary human hepatocytes; Pluronic® F127, polyethylene-polypropylene-polyethylene; PTECs, proximal tubule epithelial cells; RBL-2H3, rat basophilic leukemia cells; RPTEC, primary human renal proximal tubule epithelial cells; SA, sodium alginate; SLA, stereolithography apparatus; TBBPA, Tetrabromobisphenol A; Vas-POAC, vascularized proximal tubule-on-a-chip; μCOP, micro-continuous optical printing.

reactions. The biological complexity of its toxicity assessment models plays a pivotal role in determining the validity of toxicological predictions. Traditional 2D hepatic models are hindered by the absence of ECM-mediated polarity signals and interactions with non-parenchymal cells such as stellate and Kupffer cells, resulting in a dramatic reduction in cytochrome P450 enzyme activity—up to 80% within 72 h—severely limiting their utility in chronic toxicity studies.

In drug toxicity testing, particularly with antibiotics like trovafloxacin and its non-toxic analog levofloxacin, traditional methods have frequently failed to accurately evaluate hepatotoxicity, leading to severe consequences. Nguyen *et al.*[194] addressed this issue using 3D-printed human liver tissue models, which not only distinguished the toxicological profiles of these drugs but also maintained drug-induced cytochrome P450 enzyme activity over prolonged durations. Another study demonstrated that 3D-printed HepaRG and human stellate cell liver organoids exhibited substantially higher albumin expression compared to 2D cultures, markedly improving the sensitivity and accuracy of toxicological evaluations, thus offering a novel approach to upgrading toxicity assessment models, particularly for long-term testing.[207]

For instance, Bhise *et al.*[153] developed a 3D-bioprinted liver chip platform that preserved hepatic function for a 30-day culture period and demonstrated toxicity responses comparable to animal models and other *in vitro* systems, innovatively integrating 3D bioprinting with microfluidic bioreactors for drug toxicity assessment. He *et al.*[195] constructed a 3D-bioprinted liver tissue model derived from human induced pluripotent stem cells (hiPSCs), which exhibited exceptional performance in cell growth, liver-specific functions, and drug-induced hepatotoxic responses. This model showed excellent drug responsiveness and high cytochrome P450 1A2 expression in acetaminophen-induced hepatotoxicity tests, providing a new tool for personalized drug screening and toxicological research.

Moreover, 3D-bioprinted liver models that simulate native hepatic lobule microstructures are more sensitive and relevant in predicting drug-induced liver injuries when incorporating non-parenchymal cells, compared to hepatocyte-only models.[196] This provides pharmaceutical companies with a cost-effective and efficient platform for hepatotoxicity screening. In studies on drugs like aspirin, dexamethasone, trovafloxacin mesylate, and troglitazone, 3D-bioprinted liver models demonstrated robust intercellular communication and hepatic metabolic functions, effectively predicting hepatotoxicity and offering substantial support for toxicological screening in drug development.

In the realm of food safety testing, Wang *et al.*[130] developed a 3D-bioprinted "hepatic lobule" microtissue biosensor for aflatoxin B1 detection, combining 3D bioprinting with electrochemical sensing strategies to enhance biomimicry and accuracy, paving the way for novel approaches in mycotoxin detection. For marine biotoxin okadaic acid, researchers created an animal-free 3D-bioprinted liver model that successfully evaluated its hepatotoxicity, highlighting the efficacy of 3D bioprinting in toxicological testing and its substantial implications for long-term stability, functionality, and relevance.[197]

In environmental pollutant testing, Yao *et al.*[189] employed 3D printing to generate hiPSC-derived liver organoids (DOs) from healthy donors and alcoholic liver disease patients to assess the combined toxicity of microplastics and tetrabromobisphenol A (TBBPA), as shown in Figure 7B. Using electro-assisted inkjet printing, the study investigated the accumulation of polystyrene microplastics in DOs and the effects of TBBPA. Results indicated limited impact on DOs from healthy donors at low microplastic and TBBPA doses, whereas alcoholic liver disease patient-derived DOs exhibited heightened sensitivity, as evidenced by marked alterations in gene expression and liver function. This suggests that 3D-printed hiPSC-derived DOs represent a powerful tool for assessing the hepatic impact of environmental toxins, particularly for patients with specific genetic backgrounds.

In materials toxicology, Khanal *et al.*[198] employed scaffold-free bioprinting to fabricate a "mini-liver" model, which, combined with label-free nanoscale technology, assessed the toxicity of nanodiamonds. This model proved to be more sensitive than 2D models by detecting cytotoxicity within 48 h, providing a novel high-resolution approach to nanosafety evaluation.

4.2. Kidney toxicology

Nephrotoxicity continues to be a significant challenge in drug development and chemical safety evaluation, particularly as the renal proximal tubule serves as the primary target for drug-induced nephrotoxicity, which affects over 20% of the global adult population. However, current preclinical approaches, including 2D cell cultures and animal models, are hindered by their short-term functional maintenance *in vitro* or significant interspecies differences, limiting their ability to accurately predict clinical drug responses. The advent of 3D-bioprinted kidney models, which precisely replicate the structure of renal tubules and nephron units, has significantly enhanced the precision of toxicity predictions.

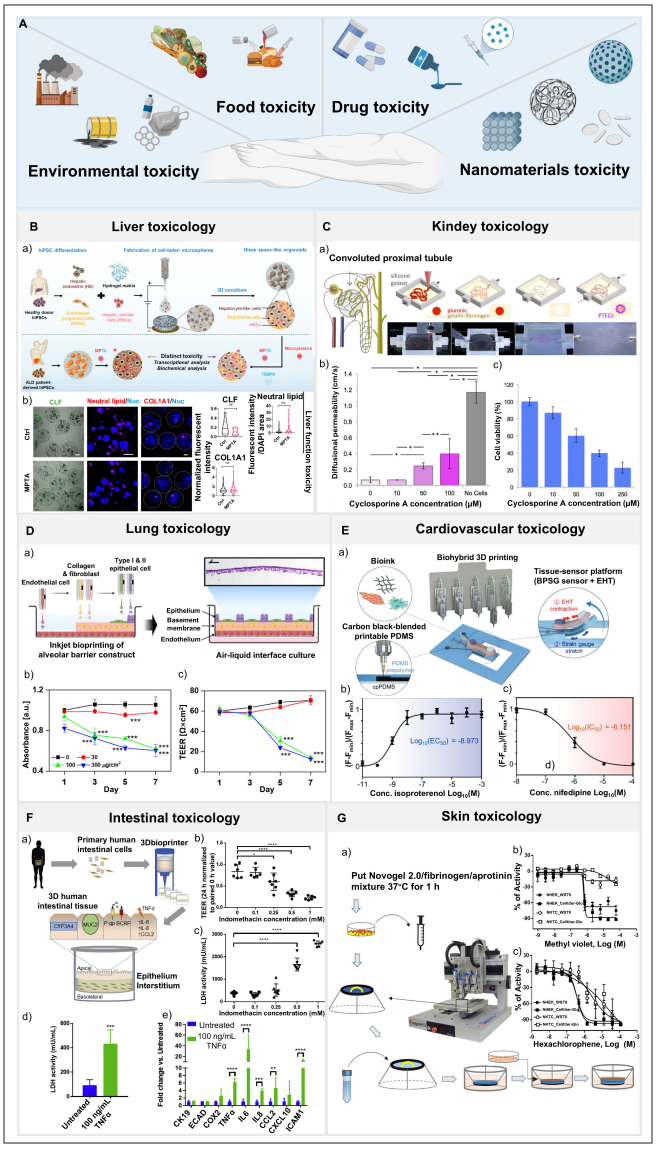

Figure 7. Applications of three-dimensional (3D) printing in organ-specific toxicology. (A) Multidimensional atlas of toxicity sources. Created with Biorender [û, NP. (2025). https://BioRender.com/5bdwv4e. (B) Differential toxicity in human induced pluripotent stem cell (hiPSC)-derived liver organoids from healthy and patient donors upon co-exposure to microplastics and tetrabromobisphenol (TBBPA). (a) Overlay of cholyl-lysyl-fluorescein (CLF) *in situ* staining (green) with bright field images. (b) Maximum projections of neutral lipid staining (red), collagen type 1 alpha chain 1 (COL1A1) immunostaining (yellow green), and 4',6-diamidino-2-phenylindole (DAPI) (blue) within microsphere-encapsulated N_Dos. Scale bar: 100 µm. Quantification of CLF uptake, lipid accumulation, and COL1A1 expression is shown below; statistical significance was assessed by Student's *t*-test ("ns" = not significant). Adapted with permission from Liang *et al.*[189] (C) 3D convoluted renal proximal tubule-on-a-chip. (a) Nephron schematic highlighting the proximal tubule and fabrication workflow using fugitive ink printed within a gelatin–fibrin extracellular matrix (ECM). (b) Diffusional permeability after cyclosporine A treatment (*$p < 0.003$, **$p < 0.02$); (c) Cell viability in a 2D dish control following cyclosporine A exposure (all comparisons $p < 0.005$). Adapted with permission from Homan *et al.*[19] (D) Toxicity assessment of dust particles in a 3D inkjet-printed alveolar barrier model: (a) Experimental workflow schematic; (b) CCK-8 proliferation assay normalized to Day 1 control (data = 1); (c) TEER measurements indicating barrier integrity after dust exposure. Adapted with permission from Kang *et al.*[190] Copyright © 2022 Wiley Periodicals LLC. (E) Tissue-sensor platform with carbon-black-blended PDMS (cpPDMS): (a) Schematic of platform fabrication; (b) Real-time contraction dose-response of engineered heart tissue (EHT) exposed to isoproterenol; (c) Real-time contraction dose-response of EHT exposed to nifedipine. Adapted with permission from Yong *et al.*[191] (F) 3D intestinal tissue model for functional and toxicity testing: (a) Workflow for tissue assembly, functional validation, and toxicity assays; (b) TEER reduction following 24 h incubation with increasing indomethacin doses; (c) LDH release correlating with indomethacin concentration; (d) Morphological changes and LDH increase after TNF-α treatment ($n = 5–6$, ***$p < 0.001$ by *t*-test); (e) Upregulation of inflammatory markers (TNF-α, IL-6, IL-8, CCL2, ICAM) in response to TNF-α ($n = 3$; **$p < 0.01$, ***$p < 0.001$, ****$p < 0.0001$ by two-way ANOVA). Data are mean ± SD. Adapted with permission from Madden *et al.*[192] (G) Full-thickness skin (FTS) model: (a) Bioprinting schematic; (b, c) Cytotoxicity evaluation of methyl violet and hexachlorophene. Adapted with permission from Wei *et al.*[193]

For instance, Homan *et al.*[19] employed an advanced 3D bioprinting technique to fabricate *in vitro* 3D human proximal tubule models, as shown in Figure 7C. These models are fully embedded within an ECM and integrated into perfusable organ-on-a-chip systems, achieving stability for up to 2 months under *in vitro* conditions. By combining 3D cell culture with organ-on-a-chip technology, the researchers created programmable, coiled proximal tubules featuring open lumens surrounded by proximal tubule epithelial cells exposed to physiological shear stress within the chip. Compared to traditional 2D cell cultures, these models exhibited considerable improvements in both morphological and functional attributes, including enhanced epithelial morphology and functional properties.

When tested with the nephrotoxic drug cyclosporin A, the 3D-bioprinted proximal tubule model successfully replicated the microarchitecture and functional characteristics of native renal tissues. The model demonstrated robust intercellular communication and renal metabolic activity, offering a robust platform for precise nephrotoxicity prediction. In comparison to 2D counterparts, the 3D model displayed higher sensitivity and correlation in drug toxicity assessments, facilitating detailed evaluation of drug-induced renal damage. This platform provides pharmaceutical companies with a cost-efficient and dependable nephrotoxicity screening platform, thereby accelerating drug development.

In addition to proximal tubule models, researchers have developed vascularized proximal tubule-on-a-chip systems (Vas-POAC), which outperform earlier single-cell proximal tubule models in replicating physiological conditions.[199] These perfusable Vas-POAC systems facilitate the growth and proliferation of proximal tubule cells alongside adjacent endothelial cells across diverse conditions. After 7 days of *in vitro* culture, Vas-POAC demonstrated mature marker expression of proximal tubule and endothelial cells in both epithelial and luminal endothelial compartments. This encompassed polarized expression of sodium-glucose cotransporter-2 and the de novo synthesis of ECM proteins. Compared to POAC systems that lack vascular components, Vas-POAC exhibited significantly enhanced functional attributes. Furthermore, in cisplatin-induced nephrotoxicity evaluations, Vas-POAC exhibited greater drug tolerance compared to POAC, highlighting its superiority in replicating physiological responses to nephrotoxic agents. These vascularized models enable the screening of drug doses responsible for proximal tubule damage and unlock new opportunities for identifying compounds that disrupt renal tubule formation.

4.3. Lung toxicology

The lungs, as the primary site for gas exchange and exposure to inhaled substances, occupy a pivotal role in toxicological studies. Airborne particulate matter entering the respiratory system through the airways can trigger severe pulmonary diseases, thereby rendering its impact analysis a focal point of research. However, traditional 2D models are significantly limited in their ability to replicate the complex physiological processes of the human body and fail to accurately simulate the effects of particulate matter on alveoli. To address these limitations, Kang *et al.*[190] employed the MicroFab Jetlab II on-demand inkjet bioprinting system to precisely deposit endothelial cells, collagen, fibroblasts, and alveolar epithelial cells onto a porous substrate at high resolution, thereby recreating the 3D, tri-layer architecture of the human alveolar barrier, as shown in Figure 7D. In this multilayer model, exposure to varying concentrations and durations of dust particles led to marked disruption of barrier integrity, induction of apoptosis, elevated secretion of pro-inflammatory cytokines, activation of key signaling pathways and transcription factors, and degradation of the ECM, culminating in increased permeability. Moreover, dust exposure altered the expression of surfactant protein genes, indicating potential impairment of alveolar surfactant function. This high-precision *in vitro* platform faithfully recapitulates *in vivo* pulmonary physiology and offers a powerful tool for particulate matter toxicology studies, accelerating the translation of findings into effective therapeutic strategies. In the field of drug toxicology, Khalid *et al.*[200] created an integrated biosensor-based lung cancer chip platform designed for real-time physiological monitoring and toxicity assessment. Constructed using 3D printing technology, the platform incorporated transparent indium tin oxide electrodes, allowing for visual monitoring via a digitally printed microscope. Optical pH sensors and transendothelial electrical resistance impedance sensors were utilized to continuously monitor the pH of the culture medium and the electrophysiological properties of cells. As a proof of concept, NCI-H1437 lung cancer cells were cultured on a glass-based microfluidic chip, with biosensor data collected in real time. The study evaluated the toxicity of two anticancer drugs, doxorubicin and docetaxel, revealing a marked increase in cell mortality with increasing drug concentrations. Doxorubicin exhibited higher toxicity compared to docetaxel, as confirmed through cell index assessments. Half-maximal inhibitory concentration values calculated via linear regression models were 6.791 μM for doxorubicin and 0.137 nM for docetaxel. Results from live/dead cell assays were consistent with transendothelial electrical resistance impedance evaluations, further validating the dose-dependent increase in cell death.

In the domain of food safety, Chandiramoha *et al.*[201] utilized 3D printing technology to create an *in vitro* exposure system (IVES) to simulate the physiological effects of cannabis inhalation on the lungs. The system was designed to load epithelial cells and expose them to cannabis smoke to mimic pulmonary responses to inhaled substances. The team fabricated a lung-like four-chamber IVES using 3D printing, featuring two inlets, four outlets, and four chamber lids, effectively simulating the "inhalation" process and distributing smoke to four cell-filled chambers before expelling it. During experiments, research-grade cannabis was ignited, with smoke introduced into the IVES via a three-way valve and syringe. Following simulated inhalation, the researchers assessed epithelial cell viability and immune function, finding a marked impairment of cellular immunity. Results revealed that cannabis use could induce symptoms such as coughing, wheezing, and chest tightness. By comparing cytokine levels in the IVES with those extracted from individuals with smoking-related disorders, the study underscored the heightened susceptibility of recreational cannabis users to throat inflammation and other respiratory issues. These findings hold particular relevance in the context of cannabis legalization for medical use. The study also emphasized the potential of 3D printing technology in toxicological research, including aerosol analysis, pathogen impact evaluations, and immune system studies.

In material toxicology, Gerbolés *et al.*[202] investigated the application of 3D bioprinting in fabricating organoid-based scaffolds for long-term NP toxicity studies. This approach aimed to better simulate lung cell exposure to NPs, providing a more accurate model compared to traditional 2D cell cultures. Using a customized 3D bioprinter, the researchers fabricated viscous hydrogels containing cells, composed of alginate, gelatin, and Matrigel, optimized to support cell viability and structural integrity. Immortalized lung cell lines were cultured within the bioprinted scaffolds over extended periods to examine interactions with NPs, including 40 nm fluorescent latex particles and 11–14 nm silver NPs. Results revealed enhanced cell proliferation within the 3D scaffolds, with cell numbers increasing from 5×10^5 to 1.27×10^6 over 14 days, indicating an optimal environment for cellular growth. Lipid peroxidation levels decreased by 91%, indicating reduced oxidative stress, a common response to NP exposure. Additionally, the 3D environment demonstrated minimal cell death over 21 days, underscoring the protective nature of the bioprinted scaffolds. NP diffusion within the 3D scaffolds was another critical observation, with fluorescent NPs permeating the scaffold, effectively replicating *in vivo* conditions. Compared to 2D cultures, cells exposed to silver NPs in the 3D model displayed significantly higher survival rates, highlighting the model's superior replication of *in vivo* NP exposure responses. The study highlighted the numerous advantages of 3D bioprinting in nanotoxicology research, including the creation of physiologically relevant models, enhanced NP diffusion and cellular interactions, and more realistic toxicity assessments. These findings suggest that 3D bioprinting could become a pivotal tool in future nanotoxicology and nanomedicine research, providing a reliable and ethical alternative to traditional methods while adhering to the 3R principles in toxicological studies.

4.4. Cardiovascular toxicology

The heart, as a key target organ for the toxicity of exogenous chemicals, is crucial in drug toxicology research. Zhang *et al.*[203] developed an innovative approach utilizing 3D bioprinting technology to construct endothelialized myocardial and heart-on-a-chip models. Using composite bioinks, the researchers created microfibrillar hydrogel scaffolds via 3D bioprinting and directly incorporated endothelial cells into these scaffolds. Over time, the endothelial cells migrated to the periphery of the microfibers, establishing a continuous endothelial layer. Subsequently, cardiomyocytes were seeded onto these 3D endothelial beds, resulting in organized myocardial tissues that exhibited spontaneous and synchronous contraction. These organoids were embedded into specially designed microfluidic perfusion bioreactors, thereby completing the endothelialized myocardial platform for cardiovascular toxicity evaluation. Using doxorubicin—a common anticancer drug—as a test case, the endothelialized myocardial tissue chip model was evaluated for its cardiovascular toxic response to the drug. Results showed that upon exposure to 10 and 100 mM doxorubicin, cardiomyocyte contraction rates decreased to 70.5% and 1.62%, respectively. Constructs exposed to 10 and 100 mM doxorubicin exhibited reductions in von Willebrand factor levels secreted by endothelial cells to 76.0% and 35.3%, respectively. These findings demonstrate that the endothelialized myocardial tissue chip model effectively simulates the dose-dependent toxic effects of doxorubicin on cardiomyocytes and endothelial cells, providing potential applications for personalized drug screening and mitigating drug-induced cardiovascular toxicity.

Concurrently, Yong *et al.*[191] created a biohybrid 3D printing method to fabricate a tissue-sensor platform, as shown in Figure 7E. This platform consists of an engineered heart tissue (EHT) integrated with dual-column-grafted strain gauge sensors, facilitating wireless, real-time, and continuous monitoring of drug-induced cardiotoxicity. Through a one-step printing process, researchers produced integrated 3D EHT and strain gauge sensors utilizing five distinct inks. By printing two

columns onto the strain gauge to serve as grafts, they increased the contraction force of the EHT and directed its self-assembly along the strain gauge. Additionally, the researchers incorporated a wireless multi-channel electronic system to continuously monitor the contraction force of the EHT, enabling the observation of both acute and chronic drug effects on the myocardium. The study demonstrated that the developed tissue-sensor platform could serve as a test model for drug-induced cardiotoxicity, validating its potential through the observation of acute and chronic effects of drugs such as isoproterenol, nicardipine, and doxorubicin. This platform provides real-time monitoring of myocardial contraction force and rhythm, providing more accurate data on drug effects compared to traditional 2D cardiac models.

In the realm of material toxicology, Miller *et al.*[204] employed advanced 3D bioprinting technology to fabricate iPSC-derived cardiac microtissues for evaluating the toxicity of copper oxide (CuO) NPs. 3D bioprinting was used to construct cardiac microtissues with structural and functional properties that closely resemble human cardiac tissue. These bioprinted tissues included iPSC-derived cardiomyocytes and human cardiac fibroblasts, thus creating a complex tissue environment. CuO NPs were coated with bovine serum albumin to mimic *in vivo* protein adsorption, thereby stabilizing the NPs and enhancing the reliability of experimental outcomes. The study found that exposure to CuO NPs led to significant cytotoxicity in the bioprinted cardiac tissues, as viability assays indicated a median lethal dose of 7.176 μg/mL and complete cell death at 100 μg/mL. Tissue contraction force was notably reduced at 10 μg/mL, underscoring the impact of CuO NPs on cardiac function. Gene expression analysis further elucidated the mechanisms of CuO NP toxicity, revealing a dose-dependent increase in markers of mitochondrial biogenesis and significant upregulation of caspase 3 and caspase 8, suggesting that apoptosis in cardiac tissues is primarily mediated through the extrinsic death receptor pathway. Compared to traditional models, 3D-bioprinted cardiac tissues offer significant advantages, such as an enhanced replication accuracy of cell-cell and cell-matrix interactions, thereby offering authentic assessments of cellular behavior and responses. Additionally, the integration of force measurement capabilities enables direct evaluation of changes in tissue contraction force, which is crucial for understanding the impact of toxins on cardiac health. These findings indicate that 3D bioprinting technology offers a powerful and precise tool for cardiac toxicology research, aiding in the elucidation of toxicity mechanisms and the development of safer materials.

4.5. Intestinal toxicology

As the primary site for drug absorption and metabolism, the small intestine is critical in toxicological testing, facilitating the evaluation of substance absorption efficiency and potential gastrointestinal toxicity.[208] The development of 3D-printed intestinal models, which accurately mimic the crypt-villus architecture, has markedly improved the physiological relevance of these models. For instance, Madden *et al.*[192] presented a 3D primary human intestinal tissue model constructed using Organovo's 3D NovoGen bioprinting system, as shown in Figure 7F. The model utilizes bioprinting technology to create a bilayered structure composed of primary human intestinal epithelial cells and intestinal myofibroblasts, effectively recapitulating key features of native intestinal tissue, including epithelial polarization, tight junctions, and specialized cell types. The engineered 3D intestinal tissue exhibits functional expression of cytochrome P450 enzymes (e.g., cytochrome P450 3A4, cytochrome P450 2C9), with demonstrated metabolic activity and inducibility. It also possesses physiologically relevant barrier properties, enabling discrimination between compounds with high and low permeability, and exhibits functional expression of key drug transporters such as P-glycoprotein and breast cancer resistance protein. In toxicity assessments, the model responds to nonsteroidal anti-inflammatory drug-induced (e.g., indomethacin) and tumor necrosis factor alpha-induced barrier disruption and cytotoxicity, supporting its utility for predicting drug safety and efficacy, rendering it particularly suitable for ADME/toxicological studies.

In another study, researchers utilized advanced biomanufacturing techniques to create three distinct intestinal barrier models: (i) a manually constructed model comprising Caco-2 and HT-29 cells on a collagen bed, (ii) a manually constructed model featuring Caco-2/HT-29 layers on an human dermal fibroblast collagen layer, and (iii) a 3D-bioprinted model incorporating both cell layers.[206] These models were rigorously tested to evaluate their capacity to simulate functional intestinal membranes. Results indicated that while all models successfully replicated the structure and function of the intestinal barrier, the 3D-bioprinted intestinal model exhibited superior epithelial barrier integrity, tight junction formation, microvilli development, and mucus production. Notably, in ibuprofen exposure experiments, the 3D-bioprinted model yielded more predictive responses, highlighting its potential as a reliable *in vitro* tool for drug toxicity testing.

In the field of food safety testing, the innovative application of mimicking "intestinal microvilli" has

demonstrated significant potential. Jiang *et al.*[205] created a biomimetic electrochemical cell sensor utilizing 3D bioprinting for the specific and highly sensitive detection of wheat gluten. The study innovatively synthesized self-assembled flower-like CuO NPs and hydrazide-functionalized multi-walled carbon nanotubes, enhancing sensor performance. Using GelMA hydrogel as the matrix, the researchers combined flower-like CuO NPs with hydrazide-functionalized multi-walled carbon nanotubes to form a conductive bio-composite hydrogel (bioink). Employing stereolithography 3D bioprinting technology, they accurately printed clustered microvilli structures of the small intestine onto screen-printed electrodes and immobilized rat basophilic leukemia cells within the gel framework.

Experimental results revealed that the bioprinted cell sensor could sensitively detect wheat gluten at a cell concentration of 1×10^6 cells/mL with a fixation time of 10 min, exhibiting a linear detection range of 0.1–0.8 ng/mL and a detection limit of 0.036 ng/mL. This 3D-bioprinted electrochemical cell sensor exhibited excellent stability and reproducibility, providing a simple yet novel approach for food safety testing. It shows promise for widespread application in food safety detection and evaluation.

4.6. Skin toxicology

As the primary barrier against external substances, the skin is essential in toxicological testing for identifying potential irritants or allergens. Manually engineered *in vitro* skin models are used to predict skin irritation, corrosion, or sensitization; however, these models face reproducibility issues and inconsistent tissue structure compared to natural tissue.[209] With the development of 3D printing technology, various bioprinting methods have emerged for skin structure reconstruction. Laser-assisted bioprinting is utilized to develop *in vitro* skin tissue.[210] Initially, layers of fibroblast/ECM bioink are printed, followed by layers of keratinocyte/ECM bioink. The resulting skin tissue can be integrated into rodent skin to facilitate wound healing. Another method combines inkjet and extrusion techniques to create full-thickness skin tissue with alternating layers of epidermal and dermal cell lines and ECM.[123] This tissue resembles human skin in terms of cell nucleus distribution and epidermal density. Exposure to 1% Triton X-100 reduces cell viability, while 5% sodium dodecyl sulfate results in complete loss of viability. Recently, a full-thickness model created via the extrusion-based method showed a native like skin structure.[211] Dermis was first fabricated by extruding bioink containing gelatin, alginate, fibrinogen, and fibroblasts, then cross-linked and cultured for 12 days. Subsequently, an epidermal keratinocyte layer was added. By Day 26 of culture, the dermis produced collagen, with evidence of dermal–epidermal junction and epidermal stratification.

Moreover, Wei *et al.*[193] conducted a systematic evaluation of various skin cell models to assess the irritant potential of topically applied compounds, as shown in Figure 7G. Initially, 2D monolayer models of primary neonatal and immortalized human keratinocytes underwent cytotoxicity testing. Then, 46 cytotoxic compounds were tested on 3D tissue models (reconstructed human epidermis and full-thickness skin) for skin irritation potential. Irritant potential was assessed by measuring tissue viability, transendothelial electrical resistance, and levels of cytokines interleukin (IL)-1α and IL-18. Results showed high-concentration irritants reduced tissue viability and transendothelial electrical resistance while increasing IL-1α secretion. At low concentrations, compounds mainly increased IL-18 secretion without affecting other parameters, suggesting potential sensitization. This study first integrated 2D cell models with 3D-bioprinted skin models for large-scale compound screening. Innovatively, it introduced markers like IL-1α and IL-18 secretion levels into the assessment. A high-throughput screening-compatible platform was developed to rapidly and efficiently evaluate the skin irritation potential of environmental chemicals, providing new tools for toxicology and enhancing the efficiency and accuracy of compound screening and chemical safety assessment.

4.7. Other organs toxicology

The application of 3D printing in toxicological research across various organs has also shown significant promise. For gastric toxicity modeling, Hsu *et al.*[212] employed digital light processing technology with flexible photocurable resin to fabricate a physiologically relevant 3D stomach model, inspired by porcine and human gastric structures, featuring realistic rugae. This model demonstrated mechanical properties and hydrophilicity comparable to native stomach tissue. Functionally, it recreated the gastric microenvironment more accurately than 2D systems: *Helicobacter pylori* exhibited enhanced antibiotic resistance due to rugae protection, while the activity of gastric cancer cells (MKN-45) was modulated by the model's flexibility and topography, providing a superior platform for drug screening and toxicity assessment. In the nervous system, Johnson *et al.*[164] developed a biomimetic 3D neural system chip using micro-extrusion bioprinting. The chip's customized microchannels and chambers enabled spatial organization of neural cells (e.g., hippocampal neurons and Schwann cells) and alignment of axonal networks. Using this platform, pseudorabies virus transmission was investigated, revealing Schwann cells' role in axon-to-cell spread and their intrinsic resistance to infection, offering a

novel tool for studying neurotropic viruses and evaluating neurotoxic compounds. Furthermore, 3D-bioprinted brain tumor models, such as glioblastoma, have been utilized to assess neurotoxicity and drug resistance (e.g., to temozolomide) by precisely replicating the tumor microenvironment.[213] In pancreatic research, Kiemen *et al.*[214] integrated serial tissue sectioning with deep learning to construct a 3D model encompassing normal ducts, pancreatic intraepithelial neoplasia, and ductal adenocarcinoma. This approach offers new insights into pancreatic cancer progression and a robust platform for evaluating drug-induced pancreatic toxicity. Collectively, these advances significantly contribute to the development of organ-specific *in vitro t*oxicology models for the stomach, nervous system, and pancreas.

5. Future perspectives and challenges

Three-dimensional bioprinting technology holds significant promise for toxicology research, yet its advancement is impeded by intricate interdisciplinary challenges. From a technical perspective, the trade-off between printing precision and throughput restricts the capacity to accurately replicate complex organ microstructures. Although photopolymerization techniques can achieve high precision, their low throughput characteristics are insufficient to address the requirements of high-throughput screening. Conversely, extrusion-based printing can significantly increase throughput, but challenges such as reduced cell viability and the inability to replicate submicron-scale physiological structures with precision persist. Additionally, the limitations of current material systems restrict the scope of the technology's application. Commercially available bioinks often lack the mechanical adaptability to match the dynamic stiffness variations of natural organs, resulting in structural collapse or functional deterioration during long-term culture, ultimately undermining model stability and reliability.

Biologically, existing models are inadequate for integrating multicellular interaction networks and systemic toxicity responses. While capable of incorporating multiple cell types, they demonstrate notable shortcomings in simulating immune microenvironments and neuroendocrine regulation. Cross-organ toxicity studies face even greater technical hurdles. For instance, in liver-gut co-culture systems, deviations in hemodynamic parameter simulations lead to drug metabolism rates that frequently deviate substantially from clinical data. Furthermore, the absence of standardized systems compounds the challenges associated with technological translation, necessitating improvements in the cross-platform comparability of key parameters to facilitate widespread application of research findings.

Future technological breakthroughs must adhere to a progressive trajectory from structural biomimicry to system integration. Innovations in multiphoton polymerization and microfluidic technologies present opportunities to address the printing bottlenecks of submicron-scale vasculature and neural networks, and to engineer smart, responsive bioinks capable of dynamically simulating tissue remodeling. The construction of multi-organ chips must incorporate physiological pharmacokinetic models and enhance cross-tissue material transfer efficiency via hydrodynamic simulations. Standardization efforts should focus on establishing batch consistency certification for bioinks and functional verification protocols, thereby promoting regulatory acceptance of printed data as partial substitutes for animal testing, ultimately expediting clinical translation.

In terms of building a translational ecosystem, a collaborative innovation network encompassing "biomanufacturing-computational toxicology-clinical medicine" needs to be established. The development of modular desktop bioprinters will effectively lower equipment barriers, while the commercialization of lyophilized bioinks is expected to significantly improve the accessibility and availability of models. The deep integration of artificial intelligence has the potential to autonomously optimize printing parameters and precisely analyze toxicity mechanisms, ultimately supporting the establishment of individualized toxicity warning systems. This technological evolution pathway is poised to transform toxicology research from empirical threshold judgments to mechanism-driven, precise prediction paradigms, providing revolutionary solutions for global public health safety.

Acknowledgments

The authors thank all the lab members for their critical reading and comments on the manuscript. They also acknowledge the Biorender platform (biorender.com) for figure illustrations.

Funding

This project was partially supported by grants from the following sources: the National Key Research and Development Program of China (No. 2022YFA1103400, 2022YFC2406704), the National Natural Science Foundation of China (No. 32371477, 82090051, 92168207), and the Research & Development Program of Zhejiang Province (No. 2024C03075 and No. 2019C04020).

Conflict of interest

The authors declare that they have no competing interests.

Author contributions

Conceptualization: Juan Liu, Yunfang Wang, Xiangdong Kong
Data curation: Yinpeng Le, Tanqing Long, Mingyue Pan, Qingru Song
Formal analysis: Yinpeng Le, Tanqing Long, Wenrui Ma, Yuxin Su
Supervision: Yunfang Wang, Xiangdong Kong
Visualization: Juan Liu, Yinpeng Le, Mengcheng Tang
Writing–original draft: Juan Liu, Yinpeng Le
Writing–review & editing: Yinpeng Le, Tanqing Long, Qi Wang, Wenrui Ma, Yuxin Su, Juan Liu, YuTian Feng, Ni An, Wenzhen Yin
All authors read and approved the final manuscript.

Ethics approval and consent to participate

Not applicable.

Consent for publication

Not applicable.

Availability of data

Not applicable.

References

1. Guengerich FP. Mechanisms of drug toxicity and relevance to pharmaceutical development. *Drug Metab Pharmacok*. 2011;26(1):3-14. doi: 10.2133/dmpk.dmpk-10-rv-062
2. Tsaioun K. Evidence-based absorption, distribution, metabolism, excretion (ADME) and its interplay with alternative toxicity methods. *ALTEX*. 2016;33:343-358. doi: 10.14573/altex.1610101
3. Pognan F, Beilmann M, Boonen HCM, *et al*. The evolving role of investigative toxicology in the pharmaceutical industry. *Nat Rev Drug Discov*. 2023;22(4):317-335. doi: 10.1038/s41573-022-00633-x
4. Ng WL, Yeong WY. The future of skin toxicology testing – three-dimensional bioprinting meets microfluidics. *IJB*. 2019;5(1):237. doi: 10.18063/ijb.v5i2.1.237
5. Worth AP, Berggren E, Prieto P. Chemicals 2.0 and why we need to bypass the gold standard in regulatory toxicology. *Altern Lab Anim*. 2025;53(1):21-25. doi: 10.1177/02611929241296328
6. Hughes B. Industry concern over EU hepatotoxicity guidance. *Nat Rev Drug Discov*. 2008;7(9):719. doi: 10.1038/nrd2677
7. Hu C, Yang S, Zhang T, *et al*. Organoids and organoids-on-a-chip as the new testing strategies for environmental toxicology-applications & advantages. *Environ Int*. 2024;184:108415. doi: 10.1016/j.envint.2024.108415
8. Bock C, Boutros M, Camp JG, *et al*. The organoid cell atlas. *Nat Biotechnol*. 2021;39(1):13-17. doi: 10.1038/s41587-020-00762-x
9. Park SB, Kim EA, Kim KY, Koh, B. Induction of toxicity in human colon cells and organoids by size- and composition-dependent road dust. *RSC Adv*. 2023;13(5):2833-2840. doi: 10.1039/D2RA07500H
10. Vinken M, Grimm D, Baatout S, *et al*. Taking the 3Rs to a higher level: replacement and reduction of animal testing in life sciences in space research. *Biotechnol Adv*. 2025;81:108574. doi: 10.1016/j.biotechadv.2025.108574
11. Markets and Markets. In Vitro Toxicology Testing Market Growth, Drivers, And Opportunities. MarketsandMarkets; 2023. Accessed May 6, 2025. https://www.marketsandmarkets.com/ Market-Reports/ in-vitro-toxicology- testing-market-209577065.html
12. Saraswathibhatla A, Indana D, Chaudhuri O. Cell–extracellular matrix mechanotransduction in 3D. *Nat Rev Mol Cell Biol*. 2023;24(7):495-516. doi: 10.1038/s41580-023-00583-1
13. Sood D, Tang-Schomer M, Pouli D, *et al*. 3D extracellular matrix microenvironment in bioengineered tissue models of primary pediatric and adult brain tumors. *Nat Commun*. 2019;10(1):4529. doi: 10.1038/s41467-019-12420-1
14. Baker BM, Chen CS. Deconstructing the third dimension: how 3D culture microenvironments alter cellular cues. *J Cell Sci*. 2012;125(Pt 13):3015-3024. doi: 10.1242/jcs.079509
15. Jang KJ, Mehr AP, Hamilton GA, *et al*. Human kidney proximal tubule-on-a-chip for drug transport and nephrotoxicity assessment. *Integr Biol (Camb)*. 2013;5(9):1119-1129. doi: 10.1039/c3ib40049b
16. Zhang B, Gao L, Ma L, Luo Y, Yang H, Cui Z. 3D bioprinting: a novel avenue for manufacturing tissues and organs. *Engineering*. 2019;5(4):777-794. doi: 10.1016/j.eng.2019.03.009
17. Horváth L, Umehara Y, Jud C, Blank F, Petri-Fink A, Rothen-Rutishauser B. Engineering an in vitro air-blood barrier by 3D bioprinting. *Sci Rep*. 2015;5(1):7974. doi: 10.1038/srep07974
18. Burke M, Carter BM, Perriman AW. Bioprinting: uncovering the utility layer-by-layer. *J 3D Print Med*. 2017;1(3):165-179. doi: 10.2217/3dp-2017-0006

19. Homan KA, Kolesky DB, Skylar-Scott MA, *et al*. Bioprinting of 3D convoluted renal proximal tubules on perfusable chips. *Sci Rep*. 2016;6(1):34845. doi: 10.1038/srep34845

20. Kang D, Hong G, An S, *et al*. Bioprinting of multiscaled hepatic lobules within a highly vascularized construct. *Small*. 2020;16(13):e1905505. doi: 10.1002/smll.201905505

21. Choudhury D, Tun HW, Wang T, Naing MW. Organ-derived decellularized extracellular matrix: a game changer for bioink manufacturing? *Trends Biotechnol*. 2018;36(8):787-805. doi: 10.1016/j.tibtech.2018.03.003

22. Kaden T, Graf K, Rennert K, Li R, Mosig AS, Raasch M. Evaluation of drug-induced liver toxicity of trovafloxacin and levofloxacin in a human microphysiological liver model. *Sci Rep*. 2023;13(1):13338. doi: 10.1038/s41598-023-40004-z

23. Michaleas SN, Laios K, Tsoucalas G, Androutsos G. Theophrastus bombastus von hohenheim (paracelsus) (1493-1541): the eminent physician and pioneer of toxicology. *Toxicol Rep*. 2021;8:411-414. doi: 10.1016/j.toxrep.2021.02.012

24. Herr HW. Percivall pott, the environment and cancer. *BJU Int*. 2011;108(4):479-481. doi: 10.1111/j.1464-410X.2011.10487.x

25. Bertomeu-Sánchez JR. Animal experiments, vital forces and courtrooms: Mateu orfila, françois magendie and the study of poisons in nineteenth-century france. *Ann Sci*. 2012;69(1):1-26. doi: 10.1080/00033790.2011.637471

26. Michaleas SN, Veskoukis AS, Samonis G, Pantos C, Androutsos G, Karamanou M. Mathieu joseph bonaventure orfila (1787-1853): the founder of modern toxicology. *Maedica (Bucur)*. 2022;17(2):532-537. doi: 10.26574/maedica.2022.17.2.532

27. Ayala RA. Welcome to the new age. Claude bernard's "introduction to the study of experimental medicine" and the shift of medical thought towards science: 150 years later. *Arch Med Res*. 2017;48(4):393-396. doi: 10.1016/j.arcmed.2017.08.006

28. An H, Sg G. Historical milestones and discoveries that shaped the toxicology sciences. *EXS*. 2009;99:1-35. doi: 10.1007/978-3-7643-8336-7_1

29. DePass LR. Alternative approaches in median lethality (LD_{50}) and acute toxicity testing. *Toxicol Lett*. 1989;49(2-3):159-170. doi: 10.1016/0378-4274(89)90030-1

30. Pillai S, Kobayashi K, Michael M, Mathai T, Sivakumar B, Sadasivan P. John william trevan's concept of median lethal dose (LD50/LC50) – more misused than used. *J Pre Clin Clin Res*. 2021;15(3):137-141. doi: 10.26444/jpccr/139588

31. Franco NH. Animal experiments in biomedical research: a historical perspective. *Animals (Basel)*. 2013;3(1):238-273. doi: 10.3390/ani3010238

32. Erhirhie EO, Ihekwereme CP, Ilodigwe EE. Advances in acute toxicity testing: Strengths, weaknesses and regulatory acceptance. *Interdiscip Toxicol*. 2018;11(1):5-12. doi: 10.2478/intox-2018-0001

33. Seidle T, Robinson S, Holmes T, *et al*. Cross-sector review of drivers and available 3Rs approaches for acute systemic toxicity testing. *Toxicol Sci*. 2010;116(2):382-396. doi: 10.1093/toxsci/kfq143

34. Botham PA. Acute systemic toxicity–prospects for tiered testing strategies. *Toxicol In Vitro*. 2004;18(2):227-230. doi: 10.1016/S0887-2333(03)00143-7

35. Mukherjee P, Roy S, Ghosh D, Nandi SK. Role of animal models in biomedical research: a review. *Lab Anim Res*. 2022;38:18. doi: 10.1186/s42826-022-00128-1

36. Khabib MNH, Sivasanku Y, Lee HB, Kumar S, Kue CS. Alternative animal models in predictive toxicology. *Toxicology*. 2022;465:153053. doi: 10.1016/j.tox.2021.153053

37. Harrison RG, Greenman MJ, Mall FP, Jackson CM. Observations of the living developing nerve fiber. *Anat Rec*. 1907;1(5):116-128. doi: 10.1002/ar.1090010503

38. Jones HW. Record of the first physician to see henrietta lacks at the johns hopkins hospital: history of the beginning of the HeLa cell line. *Am J Obstet Gynecol*. 1997;176(6):s227-s228. doi: 10.1016/S0002-9378(97)70379-X

39. Thomson JA, Itskovitz-Eldor J, Shapiro SS, *et al*. Embryonic stem cell lines derived from human blastocysts. *Science*. 1998;282(5391):1145-1147. doi: 10.1126/science.282.5391.1145

40. Martin G. Isolation of a pluripotent cell line from early mouse embryos cultured in medium conditioned by teratocarcinoma stem cells. *PNAS*. 1981;78(12):7634-7638. doi: 10.1073/pnas.78.12.7634

41. Ames BN, Lee FD, Durston WE. An improved bacterial test system for the detection and classification of mutagens and carcinogens. *PNAS*. 1973;70(3):782-786. doi: 10.1073/pnas.70.3.782

42. Zeiger E. The test that changed the world: The ames test and the regulation of chemicals. *Mutat Res Genet Toxicol Environ Mutagene*. 2019;841:43-48. doi: 10.1016/j.mrgentox.2019.05.007

43. Volpe DA. Drug-permeability and transporter assays in caco-2 and mdck cell lines. *Future Med Chem*. 2011;3(16):2063-2077. doi: 10.4155/fmc.11.149

44. Kwatra D, Budda B, Vadlapudi AD, Vadlapatla RK, Pal D, Mitra AK. Transfected mdck cell line with enhanced expression of Cyp3a4 and P-glycoprotein as a model to study their role in drug transport and metabolism. *Mol Pharm*. 2012;9(7):1877-1886.
doi: 10.1021/mp200487h

45. Garcia-Canton C, Minet E, Anadon A, Meredith C. Metabolic characterization of cell systems used in in vitro toxicology testing: lung cell system BEAS-2B as a working example. *Toxicol In Vitro*. 2013;27(6):1719-1727.
doi: 10.1016/j.tiv.2013.05.001

46. Edmondson R, Broglie JJ, Adcock AF, Yang L. Three-dimensional cell culture systems and their applications in drug discovery and cell-based biosensors. *Assay Drug Dev Technol*. 2014;12(4):207-218.
doi: 10.1089/adt.2014.573

47. Kapałczyńska M, Kolenda T, Przybyła W, *et al*. 2D and 3D cell cultures–a comparison of different types of cancer cell cultures. *Arch Med Sci*. 2018;14(4):910-919.
doi: 10.5114/aoms.2016.63743

48. Deguchi S, Shintani T, Harada K, *et al*. In vitro model for a drug assessment of cytochrome P450 family 3 subfamily a member 4 substrates using human induced pluripotent stem cells and genome editing technology. *Hepatol Commun*. 2021;5(8):1385-1399.
doi: 10.1002/hep4.1729

49. Jensen C, Teng Y. Is it time to start transitioning from 2D to 3D cell culture? *Front Mol Biosci*. 2020;7:33.
doi: 10.3389/fmolb.2020.00033

50. Astashkina AI, Mann BK, Prestwich GD, Grainger DW. Comparing predictive drug nephrotoxicity biomarkers in kidney 3-D primary organoid culture and immortalized cell lines. *Biomaterials*. 2012;33(18):4712-4721.
doi: 10.1016/j.biomaterials.2012.03.001

51. Zhao Z, Chen X, Dowbaj AM, *et al*. Organoids. *Nat Rev Methods Primers*. 2022;2:94.
doi: 10.1038/s43586-022-00174-y

52. Sato T, Vries RG, Snippert HJ, *et al*. Single Lgr5 stem cells build crypt-villus structures in vitro without a mesenchymal niche. *Nature*. 2009;459(7244):262-265.
doi: 10.1038/nature07935

53. Broda TR, McCracken KW, Wells JM. Generation of human antral and fundic gastric organoids from pluripotent stem cells. *Nat Protoc*. 2019;14(1):28-50.
doi: 10.1038/s41596-018-0080-z

54. Miller AJ, Dye BR, Ferrer-Torres D, *et al*. Generation of lung organoids from human pluripotent stem cells in vitro. *Nat Protoc*. 2019;14(2):518-540.
doi: 10.1038/s41596-018-0104-8

55. Lancaster MA, Renner M, Martin CA, *et al*. Cerebral organoids model human brain development and microcephaly. *Nature*. 2013;501(7467):373-379.
doi: 10.1038/nature12517

56. Huch M, Dorrell C, Boj SF, *et al*. In vitro expansion of single Lgr5+ liver stem cells induced by wnt-driven regeneration. *Nature*. 2013;494(7436):247-250.
doi: 10.1038/nature11826

57. Lewis-Israeli YR, Wasserman AH, Gabalski MA, *et al*. Self-assembling human heart organoids for the modeling of cardiac development and congenital heart disease. *Nat Commun*. 2021;12(1):5142.
doi: 10.1038/s41467-021-25329-5

58. Takasato M, Er PX, Chiu HS, *et al*. Erratum: kidney organoids from human iPS cells contain multiple lineages and model human nephrogenesis. *Nature*. 2016;536(7615):238.
doi: 10.1038/nature17982

59. Corrò C, Novellasdemunt L, Li VSW. A brief history of organoids. *Am J Physiol Cell Physiol*. 2020;319(1):C151-C165.
doi: 10.1152/ajpcell.00120.2020

60. Winkler AS, Cherubini A, Rusconi F, *et al*. Human airway organoids and microplastic fibers: a new exposure model for emerging contaminants. *Environ Int*. 2022;163:107200.
doi: 10.1016/j.envint.2022.107200

61. Huh D, Matthews BD, Mammoto A, Montoya-Zavala M, Hsin HY, Ingber DE. Reconstituting organ-level lung functions on a chip. *Science*. 2010;328(5986):1662-1668.
doi: 10.1126/science.1188302

62. Oleaga C, Bernabini C, Smith AST, *et al*. Multi-organ toxicity demonstration in a functional human in vitro system composed of four organs. *Sci Rep*. 2016;6(1):20030.
doi: 10.1038/srep20030

63. Liu X, Wang X, Zhang L, *et al*. 3D liver tissue model with branched vascular networks by multimaterial bioprinting. *Adv Healthc Mater*. 2021;10(23):e2101405.
doi: 10.1002/adhm.202101405

64. Xu Y, Hu Y, Liu C, Yao H, Liu B, Mi S. A novel strategy for creating tissue-engineered biomimetic blood vessels using 3D bioprinting technology. *Materials (Basel)*. 2018;11(9):1581.
doi: 10.3390/ma11091581

65. Richards D, Jia J, Yost M, Markwald R, Mei Y. 3D bioprinting for vascularized tissue fabrication. *Ann Biomed Eng*. 2017;45(1):132-147.
doi: 10.1007/s10439-016-1653-z

66. Liu J, Miller K, Ma X, *et al*. Direct 3D bioprinting of cardiac micro-tissues mimicking native myocardium. *Biomaterials*. 2020;256:120204.
doi: 10.1016/j.biomaterials.2020.120204

67. Wang Z, Wang L, Li T, *et al*. 3D bioprinting in cardiac tissue engineering. *Theranostics*. 2021;11(16):7948-7969.
doi: 10.7150/thno.61621

68. Zhou W, Yuan W, Chen Y, *et al*. Single-cell transcriptomics reveals the pulmonary inflammation induced by inhalation of subway fine particles. *J Hazard Mater*. 2024; 463:132896.
doi: 10.1016/j.jhazmat.2023.132896

69. Bai C, Wu L, Li R, Cao Y, He S, Bo X. Machine learning-enabled drug-induced toxicity prediction. *Adv Sci (Weinh)*. 2025;12(16):e2413405.
doi: 10.1002/advs.202413405

70. Guan D, Fan K, Spence I, Matthews S. Combining machine learning models of *in vitro* and *in vivo* bioassays improves rat carcinogenicity prediction. *Regul Toxicol Pharmacol*. 2018;94:8-15.
doi: 10.1016/j.yrtph.2018.01.008

71. Yavvari P, Laporte A, Elomaa L, *et al*. 3D-cultured vascular-like networks enable validation of vascular disruption properties of drugs in vitro. *Front Bioeng Biotechnol*. 2022;10:888492.
doi: 10.3389/fbioe.2022.888492

72. Berglund JD, Galis ZS. Designer blood vessels and therapeutic revascularization. *Br J Pharmacol*. 2003; 140(4):627-636.
doi: 10.1038/sj.bjp.0705457

73. Cook JC, Wu H, Aleo MD, Adkins K. Principles of precision medicine and its application in toxicology. *J Toxicol Sci*. 2018;43(10):565-577.
doi: 10.2131/jts.43.565

74. Guillemot F, Souquet A, Catros S, Guillotin B. Laser-assisted cell printing: principle, physical parameters versus cell fate and perspectives in tissue engineering. *Nanomedicine (Lond)*. 2010;5(3):507-515.
doi: 10.2217/nnm.10.14

75. Guillotin B, Catros S, Guillemot F. Laser assisted bio-printing (LAB) of cells and bio-materials based on laser induced forward transfer (LIFT). In: Schmidt V, Belegratis MR, eds. *Biological and Medical Physics, Biomedical Engineering*. Springer Berlin Heidelberg; 2014:193-209.
doi: 10.1007/978-3-642-41341-4_8

76. Ozbolat IT, Yu Y. Bioprinting toward organ fabrication: challenges and future trends. *IEEE Trans Biomed Eng*. 2013;60(3):691-699.
doi: 10.1109/TBME.2013.2243912

77. Hölzl K, Lin S, Tytgat L, Van Vlierberghe S, Gu L, Ovsianikov A. Bioink properties before, during and after 3D bioprinting. *Biofabrication*. 2016;8(3):032002.
doi: 10.1088/1758-5090/8/3/032002

78. Koch F, Tröndle K, Finkenzeller G, Zengerle R, Zimmermann S, Koltay P. Generic method of printing window adjustment for extrusion-based 3D-bioprinting to maintain high viability of mesenchymal stem cells in an alginate-gelatin hydrogel. *Bioprinting*. 2020;20:e00094.
doi: 10.1016/j.bprint.2020.e00094

79. Yin Z, Guo H, Li Y, Chiu J, Tian L. Ultrastable plasmonic bioink for printable point-of-care biosensors. *ACS Appl Mater Interfaces*. 2020;12(32):35977-35985.
doi: 10.1021/acsami.0c11799

80. Persaud A, Maus A, Strait L, Zhu D. 3D bioprinting with live cells. *Eng Regen*. 2022;3(3):292-309.
doi: 10.1016/j.engreg.2022.07.002

81. Lin H, Zhang D, Alexander PG, *et al*. Application of visible light-based projection stereolithography for live cell-scaffold fabrication with designed architecture. *Biomaterials*. 2013;34(2):331-339.
doi: 10.1016/j.biomaterials.2012.09.048

82. Dubbin K, Dong Z, Park DM, *et al*. Projection microstereolithographic microbial bioprinting for engineered biofilms. *Nano Lett*. 2021;21(3):1352-1359.
doi: 10.1021/acs.nanolett.0c04100

83. Lai J, Wang C, Wang M. 3D printing in biomedical engineering: processes, materials, and applications. *Appl Phy Rev*. 2021;8(2):021322.
doi: 10.1063/5.0024177

84. Murphy SV, Atala A. 3D bioprinting of tissues and organs. *Nat Biotechnol*. 2014;32(8):773-785.
doi: 10.1038/nbt.2958

85. Zhang J, Hu Q, Wang S, Tao J, Gou M. Digital light processing based three-dimensional printing for medical applications. *Int J Bioprint*. 2020;6(1):242.
doi: 10.18063/ijb.v6i1.242

86. Ma X, Qu X, Zhu W, *et al*. Deterministically patterned biomimetic human iPSC-derived hepatic model via rapid 3D bioprinting. *Proc Natl Acad Sci USA*. 2016;113(8): 2206-2211.
doi: 10.1073/pnas.1524510113

87. Saunders RE, Derby B. Inkjet printing biomaterials for tissue engineering: bioprinting. *Int Mater Rev*. 2014;59(8):430-448.
doi: 10.1179/1743280414Y.0000000040

88. Zhang J, Chen F, He Z, Ma Y, Uchiyama K, Lin JM. A novel approach for precisely controlled multiple cell patterning in microfluidic chips by inkjet printing and the detection of drug metabolism and diffusion. *Analyst*. 2016;141(10): 2940-2947.
doi: 10.1039/C6AN00395H

89. Gruene M, Deiwick A, Koch L, *et al*. Laser printing of stem cells for biofabrication of scaffold-free autologous grafts. *Tissue Eng Part C Methods*. 2011;17(1):79-87.
doi: 10.1089/ten.TEC.2010.0359

90. Xu T, Baicu C, Aho M, Zile M, Boland, T. Fabrication and characterization of bio-engineered cardiac pseudo tissues. *Biofabrication*. 2009;1(3):035001.
doi: 10.1088/1758-5082/1/3/035001

91. Koch L, Deiwick A, Schlie S, *et al*. Skin tissue generation by laser cell printing. *Biotechnol Bioeng*. 2012;109(7):1855-1863.
doi: 10.1002/bit.24455

92. Han W, Kong L, Xu M. Advances in selective laser sintering of polymers. *Int J Extrem Manuf*. 2022;4(4):042002. doi: 10.1088/2631-7990/ac9096

93. Duan B, Wang M, Zhou WY, Cheung WL, Li ZY, Lu WW. Three-dimensional nanocomposite scaffolds fabricated via selective laser sintering for bone tissue engineering. *Acta Biomater*. 2010;6(12):4495-4505. doi: 10.1016/j.actbio.2010.06.024

94. Jang J, Yi HG, Cho DW. 3D printed tissue models: present and future. *ACS Biomater Sci Eng*. 2016;2(10):1722-1731. doi: 10.1021/acsbiomaterials.6b00129

95. Jabbari E. Hydrogels for cell delivery. *Gels*. 2018;4(3):58. doi: 10.3390/gels4030058

96. Liu J, Wang Q, Le Y., *et al*. 3D-bioprinting for precision microtissue engineering: advances, applications, and prospects. *Adv Healthc Mater*. 2025;14(10):e2403781. doi: 10.1002/adhm.202403781

97. Zhang T, Yan KC, Ouyang L, Sun W. Mechanical characterization of bioprinted in vitro soft tissue models. *Biofabrication*. 2013;5(4):045010. doi: 10.1088/1758-5082/5/4/045010

98. Gudapati H, Yan J, Huang Y, Chrisey DB. Alginate gelation-induced cell death during laser-assisted cell printing. *Biofabrication*. 2014;6(3):035022. doi: 10.1088/1758-5082/6/3/035022

99. Li J, Wu C, Chu PK, Gelinsky M. 3D printing of hydrogels: rational design strategies and emerging biomedical applications. *Mat Sci Eng R Rep*. 2020;140:100543. doi: 10.1016/j.mser.2020.100543

100. Widhe M, Johansson U, Hillerdahl CO, Hedhammar M. Recombinant spider silk with cell binding motifs for specific adherence of cells. *Biomaterials*. 2013;34(33): 8223-8234. doi: 10.1016/j.biomaterials.2013.07.058

101. Aigner TB, DeSimone E, Scheibel T. Biomedical applications of recombinant silk-based materials. *Adv Mater*. 2018;30(19):e1704636. doi: 10.1002/adma.201704636

102. Brown M, Li J, Moraes C, Tabrizian M, Li-Jessen NYK. Decellularized extracellular matrix: new promising and challenging biomaterials for regenerative medicine. *Biomaterials*. 2022;289:121786. doi: 10.1016/j.biomaterials.2022.121786

103. Kim BS, Das S, Jang J, Cho DW. Decellularized extracellular matrix-based bioinks for engineering tissue- and organ-specific microenvironments. *Chem Rev*. 2020;120(19):10608-10661. doi: 10.1021/acs.chemrev.9b00808

104. D'souza AA, Shegokar R. Polyethylene glycol (PEG): a versatile polymer for pharmaceutical applications. *Expert Opin Drug Deliv*. 2016;13(9):1257-1275. doi: 10.1080/17425247.2016.1182485

105. Veronese FM, Pasut G. PEGylation, successful approach to drug delivery. *Drug Discov Today*. 2005;10(21): 1451-1458. doi: 10.1016/S1359-6446(05)03575-0

106. Yamaoka T, Tabata Y, Ikada Y. Distribution and tissue uptake of poly(ethylene glycol) with different molecular weights after intravenous administration to mice. *J Pharm Sci*. 1994;83(4):601-606. doi: 10.1002/jps.2600830432

107. Schmedlen RH, Masters KS, West JL. Photocrosslinkable polyvinyl alcohol hydrogels that can be modified with cell adhesion peptides for use in tissue engineering. *Biomaterials*. 2002;23(22):4325-4332. doi: 10.1016/S0142-9612(02)00177-1

108. Cheng Y, Deng S, Chen P, Ruan R. Polylactic acid (PLA) synthesis and modifications: a review. *Front Chem China*. 2009;4(3):259-264. doi: 10.1007/s11458-009-0092-x

109. Bee SL, Hamid ZAA, Mariatti M, *et al*. Approaches to improve therapeutic efficacy of biodegradable PLA/PLGA microspheres: a review. *Polym Rev*. 2018;58(3):495-536. doi: 10.1080/15583724.2018.1437547

110. Labet M, Thielemans W. Synthesis of polycaprolactone: a review. *Chem Soc Rev*. 2009;38(12):3484-3504. doi: 10.1039/B820162P

111. Kim J, Park SA, Kim J, Lee J. Fabrication and characterization of bioresorbable drug-coated porous scaffolds for vascular tissue engineering. *Materials*. 2019;12(9):1438. doi: 10.3390/ma12091438

112. Zhang W, Weng T, Li Q, *et al*. Applications of poly(caprolactone)-based nanofibre electrospun scaffolds in tissue engineering and regenerative medicine. *Curr Stem Cell Res Ther*. 2021;16(4):414-442. doi: 10.2174/1574888X15666201014145703

113. Kolesky DB, Truby RL, Gladman AS, Busbee TA, Homan KA, Lewis JA. 3D bioprinting of vascularized, heterogeneous cell-laden tissue constructs. *Adv Mater*. 2014;26(19): 3124-3130. doi: 10.1002/adma.201305506

114. Müller M, Becher J, Schnabelrauch M, Zenobi-Wong M. Nanostructured pluronic hydrogels as bioinks for 3D bioprinting. *Biofabrication*. 2015;7(3):035006. doi: 10.1088/1758-5090/7/3/035006

115. Ng WL, Yeong WY, Naing MW. Polyvinylpyrrolidone-based bio-ink improves cell viability and homogeneity during drop-on-demand printing. *Materials*. 2017; 10(2):190. doi: 10.3390/ma10020190

116. Xiang Y, Miller K, Guan J, Kiratitanaporn W, Tang M, Chen S. 3D bioprinting of complex tissues in vitro: State-

of-the-art and future perspectives. *Arch Toxicol*. 2022;96(3): 691-710.
doi: 10.1007/s00204-021-03212-y

117. Szűcs D, Fekete Z, Guba M, *et al*. Toward better drug development: three-dimensional bioprinting in toxicological research. *Int J Bioprint*. 2023;9(2):663.
doi: 10.18063/ijb.v9i2.663

118. Jain P, Kathuria H, Dubey N. Advances in 3D bioprinting of tissues/organs for regenerative medicine and in-vitro models. *Biomaterials*. 2022;287:121639.
doi: 10.1016/j.biomaterials.2022.121639

119. Wu X, Shi W, Liu X, Gu Z. Recent advances in 3D-printing-based organ-on-a-chip. *EngMedicine*. 2024;1(1):100003.
doi: 10.1016/j.engmed.2024.100003

120. Yoon S, Kilicarslan YD, Jeong U, *et al*. Microfluidics in high-throughput drug screening: Organ-on-a-chip and C. elegans-based innovations. *Biosensors*. 2024;14(1):55.
doi: 10.3390/bios14010055

121. Fuchs S, Johansson S, Tjell AØ, Werr G, Mayr T, Tenje M. In-line analysis of organ-on-chip systems with sensors: integration, fabrication, challenges, and potential. *ACS Biomater Sci Eng*. 2021;7(7):2926-2948.
doi: 10.1021/acsbiomaterials.0c01110

122. Zafeiris K, Brasinika D, Karatza A, *et al*. Additive manufacturing of hydroxyapatite–chitosan–genipin composite scaffolds for bone tissue engineering applications. *Mat Sci Eng C*. 2021;119:111639.
doi: 10.1016/j.msec.2020.111639

123. Lee V, Singh G, Trasatti JP, *et al*. Design and fabrication of human skin by three-dimensional bioprinting. *Tissue Eng Part C Methods*. 2014;20(6):473-484.
doi: 10.1089/ten.tec.2013.0335

124. Xu T, Zhao W, Zhu JM, Albanna MZ, Yoo JJ, Atala A. Complex heterogeneous tissue constructs containing multiple cell types prepared by inkjet printing technology. *Biomaterials*. 2013;34(1):130-139.
doi: 10.1016/j.biomaterials.2012.09.035

125. Jodat YA, Kiaee K, Vela Jarquin D, *et al*. A 3D-printed hybrid nasal cartilage with functional electronic olfaction. *Adv Sci*. 2020;7(5):1901878.
doi: 10.1002/advs.201901878

126. Wang Z, Abdulla R, Parker B, Samanipour R, Ghosh S, Kim K. A simple and high-resolution stereolithography-based 3D bioprinting system using visible light crosslinkable bioinks. *Biofabrication*. 2015;7(4):045009.
doi: 10.1088/1758-5090/7/4/045009

127. Anada T, Pan CC, Stahl AM, *et al*. Vascularized bone-mimetic hydrogel constructs by 3D bioprinting to promote osteogenesis and angiogenesis. *IJMS*. 2019; 20(5):1096.
doi: 10.3390/ijms20051096

128. Yin M, Yao M, Gao S, Zhang AP, Tam H, Wai PA. Rapid 3D patterning of poly(acrylic acid) ionic hydrogel for miniature pH sensors. *Adv Mater*. 2016;28(7):1394-1399.
doi: 10.1002/adma.201504021

129. Kanaki Z, Chandrinou C, Orfanou IM, *et al*. Laser-induced forward transfer printing on microneedles for transdermal delivery of gemcitabine. *IJB*. 2022;8(2):554.
doi: 10.18063/ijb.v8i2.554

130. Wang L, Cao H, Jiang H, Fang Y, Jiang D. A novel 3D bio-printing "liver lobule" microtissue biosensor for the detection of AFB1. *Food Res Int*. 2023;168:112778.
doi: 10.1016/j.foodres.2023.112778

131. Shrestha J, Ghadiri M, Shanmugavel M, *et al*. A rapidly prototyped lung-on-a-chip model using 3D-printed molds. *Organs-on-a-Chip*. 2019;1:100001.
doi: 10.1016/j.ooc.2020.100001

132. Yu C, Ma X, Zhu W, *et al*. Scanningless and continuous 3D bioprinting of human tissues with decellularized extracellular matrix. *Biomaterials*. 2019;194:1-13.
doi: 10.1016/j.biomaterials.2018.12.009

133. Zhang JXJ, Hoshino K. Nanomaterials for molecular sensing. *Molecular Sensors and Nanodevices: Principles, Designs and Applications in Biomedical Engineering*. Academic Press; 2019:413-487 .
doi: 10.1016/b978-0-12-814862-4.00007-7

134. Pan C, Xu J, Gao Q, *et al*. Sequentially suspended 3D bioprinting of multiple-layered vascular models with tunable geometries for in vitro modeling of arterial disorders initiation. *Biofabrication*. 2023;15(4):045017.
doi: 10.1088/1758-5090/aceffa

135. Song KH, Highley CB, Rouff A, Burdick JA. Complex 3D-printed microchannels within cell-degradable hydrogels. *Adv Funct Mater*. 2018;28(31):1801331.
doi: 10.1002/adfm.201801331

136. Tonti OR, Larson H, Lipp SN, *et al*. Tissue-specific parameters for the design of ECM-mimetic biomaterials. *Acta Biomater*. 2021;132:83-102.
doi: 10.1016/j.actbio.2021.04.017

137. Ma X, Liu J, Zhu W., *et al*. 3D bioprinting of functional tissue models for personalized drug screening and in vitro disease modeling. *Adv Drug Deliver Rev*. 2018;132: 235-251.
doi: 10.1016/j.addr.2018.06.011

138. Almutary AG, Alnuqaydan AM, Almatroodi SA, Bakshi HA, Chellappan DK, Tambuwala MM. Development of 3D-bioprinted colitis-mimicking model to assess epithelial barrier function using albumin nano-encapsulated anti-inflammatory drugs. *Biomimetics*. 2023;8(1):41.
doi: 10.3390/biomimetics8010041

139. Kim BS, Ahn M, Cho WW, Gao G, Jang J, Cho DW. Engineering of diseased human skin equivalent using 3D cell printing for representing pathophysiological

hallmarks of type 2 diabetes in vitro. *Biomaterials*. 2021; 272:120776.
doi: 10.1016/j.biomaterials.2021.120776

140. Vázquez-Aristizabal P, Henriksen-Lacey M, García-Astrain C, *et al*. Biofabrication and monitoring of a 3D printed skin model for melanoma. *Adv Healthc Mater*. 2024;13(27):e2401136.
doi: 10.1002/adhm.202401136

141. Tijore A, Irvine SA, Sarig U, Mhaisalkar P, Baisane V, Venkatraman S. Contact guidance for cardiac tissue engineering using 3D bioprinted gelatin patterned hydrogel. *Biofabrication*. 2018;10(2):025003.
doi: 10.1088/1758-5090/aaa15d

142. Melhem MR, Park J, Knapp L, *et al*. 3D printed stem-cell-laden, microchanneled hydrogel patch for the enhanced release of cell-secreting factors and treatment of myocardial infarctions. *ACS Biomater Sci Eng*. 2017;3(9):1980-1987.
doi: 10.1021/acsbiomaterials.6b00176

143. Ong CS, Fukunishi T, Zhang H, *et al*. Biomaterial-free three-dimensional bioprinting of cardiac tissue using human induced pluripotent stem cell derived cardiomyocytes. *Sci Rep*. 2017;7(1):4566.
doi: 10.1038/s41598-017-05018-4

144. Arai K, Murata D, Takao S, Verissiomo AR, Nakayama K. Cryopreservation method for spheroids and fabrication of scaffold-free tubular constructs. *PLoS One*. 2020;15(4):e0230428.
doi: 10.1371/journal.pone.0230428

145. Arai K, Kitsuka T, Nakayama K. Scaffold-based and scaffold-free cardiac constructs for drug testing. *Biofabrication*. 2021;13(4):1-14.
doi: 10.1088/1758-5090/ac1257

146. Mironov V, Boland T, Trusk T, Forgacs G, Markwald RR. Organ printing: computer-aided jet-based 3D tissue engineering. *Trends Biotechnol*. 2003;21(4):157-161.
doi: 10.1016/S0167-7799(03)00033-7

147. Utama RH, Atapattu L, O'Mahony AP, *et al*. A 3D bioprinter specifically designed for the high-throughput production of matrix-embedded multicellular spheroids. *iScience*. 2020;23(10):101621.
doi: 10.1016/j.isci.2020.101621

148. Matsusaki M, Sakaue K, Kadowaki K, Akashi M. Three-dimensional human tissue chips fabricated by rapid and automatic inkjet cell printing. *Adv Healthc Mater*. 2013;2(4):534-539.
doi: 10.1002/adhm.201200299

149. Gale, B.K., Jafek, A.R., Lambert, C.J., *et al*. A review of current methods in microfluidic device fabrication and future commercialization prospects. *Inventions*. 2018; 3(3):60.
doi: 10.3390/inventions3030060

150. Wu J, Gu M. Microfluidic sensing: state of the art fabrication and detection techniques. *J Biomed Opt*. 2011; 16(8):080901.
doi: 10.1117/1.3607430

151. Wu Q, Liu J, Wang X, *et al*. Organ-on-a-chip: Recent breakthroughs and future prospects. *Biomed Eng Online*. 2020;19(1):9.
doi: 10.1186/s12938-020-0752-0

152. Mehrotra S, de Melo BAG, Hirano M, *et al*. Nonmulberry silk based ink for fabricating mechanically robust cardiac patches and endothelialized myocardium-on-a-chip application. *Adv Funct Mater*. 2020;30(12): 1907436.
doi: 10.1002/adfm.201907436

153. Bhise NS, Manoharan V, Massa S, *et al*. A liver-on-a-chip platform with bioprinted hepatic spheroids. *Biofabrication*. 2016;8(1):014101.
doi: 10.1088/1758-5090/8/1/014101

154. Park JY, Ryu H, Lee B, *et al*. Development of a functional airway-on-a-chip by 3D cell printing. *Biofabrication*. 2018;11(1):015002.
doi: 10.1088/1758-5090/aae545

155. Chang R, Emami K, Wu H, Sun W. Biofabrication of a three-dimensional liver micro-organ as an in vitro drug metabolism model. *Biofabrication*. 2010;2(4): 045004.
doi: 10.1088/1758-5082/2/4/045004

156. Chang R, Nam J, Sun W. Direct cell writing of 3D microorgan for in vitro pharmacokinetic model. *Tissue Eng Part C Methods*. 2008;14(2):157-166.
doi: 10.1089/ten.tec.2007.0392

157. Lee H, Cho DW. One-step fabrication of an organ-on-a-chip with spatial heterogeneity using a 3D bioprinting technology. *Lab Chip*. 2016;16(14):2618-2625.
doi: 10.1039/C6LC00450D

158. Lin NYC, Homan KA, Robinson SS, *et al*. Renal reabsorption in 3D vascularized proximal tubule models. *PNAS*. 2019;116(12):5399-5404.
doi: 10.1073/pnas.1815208116

159. Fritschen A, Lindner N, Scholpp S, *et al*. High-scale 3D-bioprinting platform for the automated production of vascularized organs-on-a-chip. *Adv Healthc Mater*. 2024;13(17):2304028.
doi: 10.1002/adhm.202304028

160. Zhang YS, Davoudi F, Walch P, *et al*. Bioprinted thrombosis-on-a-chip. *Lab Chip*. 2016;16(21):4097-4105.
doi: 10.1039/C6LC00380J

161. Abudupataer M, Chen N, Yan S, *et al*. Bioprinting a 3D vascular construct for engineering a vessel-on-a-chip. *Biomed Microdevices*. 2019;22(1):10.
doi: 10.1007/s10544-019-0460-3

162. Cao X, Ashfaq R, Cheng F, *et al*. A tumor-on-a-chip system with bioprinted blood and lymphatic vessel pair. *Adv Funct Mater*. 2019;29(31):1807173. doi: 10.1002/adfm.201807173

163. Xie M, Gao Q, Fu J, Chen Z, He Y. Bioprinting of novel 3D tumor array chip for drug screening. *Bio-des Manuf*. 2020;3(3):175-188. doi: 10.1007/s42242-020-00078-4

164. Johnson BN, Lancaster KZ, Hogue IB, *et al*. 3D printed nervous system on a chip. *Lab Chip*. 2016;16(8):1393-1400. doi: 10.1039/C5LC01270H

165. Skardal A, Murphy SV, Devarasetty M, *et al*. Multi-tissue interactions in an integrated three-tissue organ-on-a-chip platform. *Sci Rep*. 2017;7(1):8837. doi: 10.1038/s41598-017-08879-x

166. Elezoglou E, Chliara M, Chatzipetrou M, *et al*. Laser bioprinting of cells and tumor organoids for organ-on-chip applications. In: *Frontiers in Ultrafast Optics: Biomedical, Scientific, and Industrial Applications XXIII*. Vol PC12411. SPIE; 2023:PC1241107. doi: 10.1117/12.2648068

167. Bowser DA, Moore MJ. Biofabrication of neural microphysiological systems using magnetic spheroid bioprinting. *Biofabrication*. 2019;12(1):015002. doi: 10.1088/1758-5090/ab41b4

168. Han T, Kundu S, Nag A, Xu Y. 3D printed sensors for biomedical applications: a review. *Sensors*. 2019; 19(7):1706. doi: 10.3390/s19071706

169. Cagnani GR, Ibáñez-Redín G, Tirich B, Gonçalves D, Balogh DT, Oliveira ON. Fully-printed electrochemical sensors made with flexible screen-printed electrodes modified by roll-to-roll slot-die coating. *Biosens Bioelectron*. 2020;165:112428. doi: 10.1016/j.bios.2020.112428

170. Wang R, Zhu X, Sun L, *et al*. Cost-effective fabrication of transparent strain sensors via micro-scale 3D printing and imprinting. *Nanomaterials*. 2021;12(1):120. doi: 10.3390/nano12010120

171. Wu D, Peng Q, Wu S, *et al*. A simple graphene NH3 gas sensor via laser direct writing. *Sensors*. 2018; 18(12):4405. doi: 10.3390/s18124405

172. Hecht L, Rager K, Davidonis M, Weber P, Gauglitz G, Dietzel A. Blister-actuated LIFT printing for multiparametric functionalization of paper-like biosensors. *Micromachines*. 2019;10(4):221. doi: 10.3390/mi10040221

173. Cao L, Han GC, Xiao H, Chen Z, Fang C. A novel 3D paper-based microfluidic electrochemical glucose biosensor based on rGO-TEPA/PB sensitive film. *Anal Chim Acta*. 2020;1096:34-43. doi: 10.1016/j.aca.2019.10.049

174. López Marzo AM, Mayorga-Martinez CC, Pumera M. 3D-printed graphene direct electron transfer enzyme biosensors. *Biosens Bioelectron*. 2020;151:111980. doi: 10.1016/j.bios.2019.111980

175. Lee J, Maji S, Lee H. Fabrication and integration of a low-cost 3D printing-based glucose biosensor for bioprinted liver-on-a-chip. *Biotechnol J*. 2023;18(12):e2300154. doi: 10.1002/biot.202300154

176. Guo X, Wang Z, Hou J, *et al*. A novel magnetoelastic biosensor consisting of carbon quantum dots/nitrocellulose membranes and $NiFe_2O_4$/ polylactic acid based on 3D printing for α2-macroglobulin detection. *Chin J Anal Chem*. 2024;52(9):100420. doi: 10.1016/j.cjac.2024.100420

177. Sun D, Gao W, Hu H, Zhou S. Why 90% of clinical drug development fails and how to improve it? *Acta Pharm Sin B*. 2022;12(7):3049-3062. doi: 10.1016/j.apsb.2022.02.002

178. Li X, Zhang R, Zhao B, Lossin C, Cao Z. Cardiotoxicity screening: a review of rapid-throughput in vitro approaches. *Arch Toxicol*. 2016;90(8):1803-1816. doi: 10.1007/s00204-015-1651-1

179. Muir DCG, Getzinger GJ, McBride M, Ferguson PL. How many chemicals in commerce have been analyzed in environmental media? A 50 year bibliometric analysis. *Environ Sci Technol*. 2023;57(25):9119-9129. doi: 10.1021/acs.est.2c09353

180. Godoy P, Hewitt NJ, Albrecht U, *et al*. Recent advances in 2D and 3D in vitro systems using primary hepatocytes, alternative hepatocyte sources and non-parenchymal liver cells and their use in investigating mechanisms of hepatotoxicity, cell signaling and ADME. *Arch Toxicol*. 2013;87(8):1315-1530. doi: 10.1007/s00204-013-1078-5

181. Scharff RL. Economic burden from health losses due to foodborne illness in the united states. *J Food Prot*. 2012;75(1):123-131. doi: 10.4315/0362-028X.JFP-11-058

182. Hussain MA, Dawson CO. Economic impact of food safety outbreaks on food businesses. *Foods*. 2013;2(4):585-589. doi: 10.3390/foods2040585

183. Van Norman GA. Limitations of animal studies for predicting toxicity in clinical trials: is it time to rethink our current approach? *JACC: Basic Transl Sci*. 2019;4(7): 845-854. doi: 10.1016/j.jacbts.2019.10.008

184. Monteiro-Riviere NA. Perspectives of nanotoxicology: introduction. *Wiley Interdiscip Rev Nanomed Nanobiotechnol*. 2022;14(6):e1843. doi: 10.1002/wnan.1843

185. Johnston LJ, Gonzalez-Rojano N, Wilkinson KJ, Xing B. Key challenges for evaluation of the safety of engineered nanomaterials. *NanoImpact*. 2020;18:100219. doi: 10.1016/j.impact.2020.100219

186. Clark KA, White RH, Silbergeld EK. Predictive models for nanotoxicology: current challenges and future opportunities. *Regul Toxicol Pharmacol*. 2011;59(3):361-363. doi: 10.1016/j.yrtph.2011.02.002

187. Yi HG, Kim H, Kwon J, Choi YJ, Jang J, Cho DW. Application of 3D bioprinting in the prevention and the therapy for human diseases. *Sig Transduct Target Ther*. 2021; 6(1):1-17. doi: 10.1038/s41392-021-00566-8

188. Blaeser A, Duarte Campos DF, Puster U, Richtering W, Stevens MM, Fischer H. Controlling shear stress in 3D bioprinting is a key factor to balance printing resolution and stem cell integrity. *Adv Healthc Mater*. 2016;5(3):326-333. doi: 10.1002/adhm.201500677

189. Liang S, Luo Y, Su Y, *et al*. Distinct toxicity of microplastics/ TBBPA co-exposure to bioprinted liver organoids derived from hiPSCs of healthy and patient donors. *IJB*. 2024;10(3):1403. doi: 10.36922/ijb.1403

190. Kang D, Lee H, Jung S. Use of a 3D inkjet-printed model to access dust particle toxicology in the human alveolar barrier. *Biotechnol Bioeng*. 2022;119(12):3668-3677. doi: 10.1002/bit.28220

191. Yong U, Kim D, Kim H, *et al*. Biohybrid 3D printing of a tissue-sensor platform for wireless, real-time, and continuous monitoring of drug-induced cardiotoxicity. *Adv Mater*. 2023;35(11):2208983. doi: 10.1002/adma.202208983

192. Madden LR, Nguyen TV, Garcia-Mojica S, *et al*. Bioprinted 3D primary human intestinal tissues model aspects of native physiology and ADME/Tox Functions. *iScience*. 2018;2:156-167. doi: 10.1016/j.isci.2018.03.015

193. Wei Z, Liu X, Ooka M, *et al*. Two-dimensional cellular and three-dimensional bio-printed skin models to screen topical-use compounds for irritation potential. *Front Bioeng Biotechnol*. 2020;8:109. doi: 10.3389/fbioe.2020.00109

194. Nguyen DG, Funk J, Robbins JB, *et al*. Bioprinted 3D primary liver tissues allow assessment of organ-level response to clinical drug induced toxicity in vitro. *PLoS One*. 2016;11(7):e0158674. doi: 10.1371/journal.pone.0158674

195. He J, Wang J, Pang Y, *et al*. Bioprinting of a hepatic tissue model using humaninduced pluripotent stem cell-derived hepatocytes for drug-induced hepatotoxicity evaluation. *IJB*. 2022;8(3):581. doi: 10.18063/ijb.v8i3.581

196. Janani G, Priya S, Dey S, Mandal BB. Mimicking native liver lobule microarchitecture in vitro with parenchymal and non-parenchymal cells using 3D bioprinting for drug toxicity and drug screening applications. *ACS Appl Mater Interfaces*. 2022;14(8):10167-10186. doi: 10.1021/acsami.2c00312

197. Ali ASM, Berg J, Roehrs V, *et al*. Xeno-free 3D bioprinted liver model for hepatotoxicity assessment. *Int J Mol Sci*. 2024;25(3):1811. doi: 10.3390/ijms25031811

198. Khanal D, Zhang F, Song Y, *et al*. Biological impact of nanodiamond particles – label free, high-resolution methods for nanotoxicity assessment. *Nanotoxicology*. 2019;13(9):1210-1226. doi: 10.1080/17435390.2019.1650970

199. Singh NK, Kim JY, Jang J, Kim YK, Cho DW. 3D cell printing of advanced vascularized proximal tubule-on-a-chip for drug induced nephrotoxicity advancement. *ACS Appl Bio Mater*. 2023;6(9):3750-3758. doi: 10.1021/acsabm.3c00421

200. Khalid MAU, Kim YS, Ali M, Lee BG, Cho YJ, Choi KH. A lung cancer-on-chip platform with integrated biosensors for physiological monitoring and toxicity assessment. *Biochem Engi J*. 2020;155:107469. doi: 10.1016/j.bej.2019.107469

201. Chandiramohan A, Dabaghi M, Aguiar JA, *et al*. Development and validation of an open-source, disposable, 3D-printed *in vitro* environmental exposure system for transwell culture inserts. *ERJ Open Res*. 2021;7(1):00705-02020. doi: 10.1183/23120541.00705-2020

202. Gerbolés AG, Galetti M, Rossi S, *et al*. Three-dimensional bioprinting of organoid-based scaffolds (OBST) for long-term nanoparticle toxicology investigation. *IJMS*. 2023;24(7):6595. doi: 10.3390/ijms24076595

203. Zhang YS, Arneri A, Bersini S, *et al*. Bioprinting 3D microfibrous scaffolds for engineering endothelialized myocardium and heart-on-a-chip. *Biomaterials*. 2016;110:45-59. doi: 10.1016/j.biomaterials.2016.09.003

204. Miller KL, Sit I, Xiang Y, *et al*. Evaluation of CuO nanoparticle toxicity on 3D bioprinted human iPSC-derived cardiac tissues. *Bioprinting*. 2023;32:e00284. doi: 10.1016/j.bprint.2023.e00284

205. Jiang D, Sheng K, Jiang H, Wang L. A biomimetic "intestinal microvillus" cell sensor based on 3D bioprinting for the detection of wheat allergen gliadin. *Bioelectrochemistry*. 2021;142:107919. doi: 10.1016/j.bioelechem.2021.107919

206. Tofani LB, Avelino TM, De Azevedo RJ, *et al*. Biofabricated 3D intestinal models as an alternative to animal based approaches for drug toxicity assays. *Tissue Eng Regen Med*. 2025;22(2):181-194.

doi: 10.1007/s13770-024-00694-6

207. Cuvellier M, Ezan F, Oliveira H, *et al*. 3D culture of HepaRG cells in GelMa and its application to bioprinting of a multicellular hepatic model. *Biomaterials*. 2021;269:120611. doi: 10.1016/j.biomaterials.2020.120611

208. Nguyen DG, Pentoney SL. Bioprinted three dimensional human tissues for toxicology and disease modeling. *Drug Discov Today Technol*. 2017;23:37-44. doi: 10.1016/j.ddtec.2017.03.001

209. Mathes SH, Ruffner H, Graf-Hausner U. The use of skin models in drug development. *Adv Drug Deliv Rev*. 2014;69-70:81-102. doi: 10.1016/j.addr.2013.12.006

210. Michael S, Sorg H, Peck CT, *et al*. Tissue engineered skin substitutes created by laser-assisted bioprinting form skin-like structures in the dorsal skin fold chamber in mice. *PLoS One*. 2013;8(3):e57741. doi: 10.1371/journal.pone.0057741

211. Pourchet LJ, Thepot A, Albouy M, *et al*. Human skin 3D bioprinting using scaffold-free approach. *Adv Healthc Mater*. 2017;6(4):1601101. doi: 10.1002/adhm.201601101

212. Hsu YT, Lee SP, Li CH, Ho MH, Kao CY. Preparation of 3D-printed gastric models with biomimetic mechanical, topographical and fluid dynamic properties. *J Taiwan Inst Chem Eng*. 2024;160:105389. doi: 10.1016/j.jtice.2024.105389

213. Ozbek II, Saybasili H, Ulgen KO. Applications of 3D bioprinting technology to brain cells and brain tumor models: special emphasis to glioblastoma. *ACS Biomater Sci Eng*. 2024;10(5):2616-2635. doi: 10.1021/acsbiomaterials.3c01569

214. Kiemen AL, Forjaz A, Sousa R, *et al*. High-resolution 3D printing of pancreatic ductal microanatomy enabled by serial histology. *Adv Mater Technol*. 2024;9(6):2301837. doi: 10.1002/admt.202301837